HYDROGENATION OF CARBON DIOXIDE IN A FLUIDIZED BED REACTOR

M.Sc. Thesis

Rabindra Nath Mondal
Chemical Engineering Department
Bangladesh University of Engineering & Technology
Dhaka-1000.

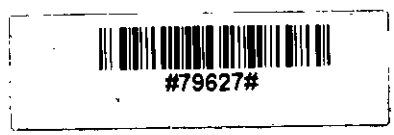

BANGLADESH UNIVERSITY OF ENGINEERING AND TECHNOLOGY
DEPARTMENT OF CHEMICAL ENGINEERING

CERTIFICATION OF THESIS WORK

We, the undersigned, certify that RABINDRA NATH MONDAL candidate for the degree of Master of Science in Engineering (Chemical) has presented his thesis on the subject "HYDROGENATION OF CARBON DIOXIDE IN A FLUIDIZED BED REACTOR" that the thesis is acceptable in form and content, and that the student demonstrated a satisfactory knowledge of the field covered by this thesis in the oral examination held on the 31st December, 1990.

(Dr. Khaliq Ahmed) — Chairman
Assistant Professor
Department of Chemical Engineering
BUET, Dhaka-1000.

(Dr. K. Ikhtyar Omar) — Member
Professor and Head,
Department of Chemical Engineering
BUET, Dhaka-1000.

(Dr. Ijaz Hossain) — Member
Assistant Professor
Department of Chemical Engineering
BUET, Dhaka-1000.

(Dr. Jasimuz Zaman) — Member
Professor
Department of Chemical Engineering
BUET, Dhaka-1000.

(Mr. Amirul Haque) — External Member
Chief Operation Manager
Chittagong Urea Fertilizer Limited
Chittagong.

ABSTRACT

A fluidized bed reactor suitable for studying heterogeneous gas-solid reactions at ambient pressures and at elevated temperatures has been constructed. The facility developed is particularly useful for studying catalytic and non-catalytic reactions under a wide range of operating conditions. To demonstrate the usefulness of the reactor, hydrogenation of CO_2 over alumina supported nickel catalyst has been studied under varying conditions of temperature, composition of reactant mixture, reduction conditions and flow rate.

Conversion of carbon dioxide to methane was found to increase continually from 210°C to 300°C but the rate of this increase in conversion dropped from 240°C onwards. Carbon dioxide concentration in the reactant mixture was varied from 2.6% to 7.8% and the feed flow rate was varied from 424 ml/min to 1192 ml/min corresponding to superficial fluidizing velosity of 1.4 cm/sec to 4.0 cm/sec. Results have been compared with those obtained in fixed bed reactor by other researchers. Fixed bed reactor literature show that there is an effect of flow on conversion whereas in this work it was found that flowrate has no effect on the conversion. Conversion achieved in the present study were found to be higher than conversion reported for fixed bed reactors for similar conditions of temperature and composition.

ACKNOWLEDGEMENT

The author acknowledges with gratitude the continuous guidance, advice, help and encouragement provided by Dr. Khaliq Ahmed and Dr. Ijaz Hossain during the course of this work. Working under their supervision was pleasant and rewarding. My sincere thanks to them for all their kind help.

The author also acknowledges with thanks the advice and suggestions of Prof. Jasimuz Zaman. The author is also grateful to Dr. Dil Afroza Begum for her kind help and co-operation during the experimental work.

Mr. Md. Shamsur Rahman, Laboratory Technician, deserves thanks for his kind help at different stages of the work. Thanks are also due to Mr. Md. Hossain Ali for typing the thesis.

CONTENTS

CHAPTER-ONE

1. Introduction:

Methanation, the hydrogenation of carbon oxides to methane, has been the subject of a large number of catalytic studies during the past seventy years. Crude hydrogen or ammonia synthesis gas produced by hydrogen/steam reforming or partial oxidation of hydrocarbons, followed by CO shift and absorption of CO_2, still contains about 0.5% of carbon oxides. These impurities are usually removed by hydrogenation to methane on a supported nickel catalyst to avoid poisoning of the catalysts used in subsequent processes such as the synthesis of ammonia. The stoichiometric equation involved are:

$$CO+3H_2 \longrightarrow CH_4+H_2O$$

$$CO_2+4H_2 \longrightarrow CH_4+2H_2O$$

Studies on rate of hydrogenation of carbon monoxide, carbon dioxide and also the mixture of CO and CO_2 are needed to evaluate the process and to design the equipment properly. Recent interest in methanation reaction is a result of this reaction being required as the final step in the production of substitute natural gas (SNG) from coal. The practical significance of this process will no doubt hinge on the creditability predicted for the severe shortages of natural gas for the imminent future. Increasing demand for natural gas as a fuel and chemical raw material, coupled with chemical gas reserves, has focused considerable interest on utilizing the

tremendous coal reserves as a possible source of gaseous fuel. An attractive process for the production of gaseous fuel from coal involves the preparation of synthesis gas containing carbon monoxide and carbon dioxide, by the reaction of coal with oxygen and superheated steam and the subsequent catalytic hydrogenation of the gas to methane and other hydrocarbons. Studies on the rate of hydrogenation of carbon monoxide and carbon dioxide are needed for this purpose.

Most of the previous work (1,2,5,6,14,15) on methanation has been expended in the study of the reactions using various catalysts as well as different types of reactors. In the earlier works(5), nickel was found to be a very efficient catalyst. Nickel is still the material of choice in most investigations of methanation, although, ruthenium, cobalt and iron are also active. Nickel catalysts were used for methanation in supported form, usually on acid washed kieselguhr or on alumina. The reactors were mainly fixed catalytic bed reactor.

In the present investigation, the reactions between hydrogen and carbon dioxide that produce methane and water was studied in a fluidized bed reactor. The catalyst used was a alumina supported nickel catalyst. The effect of temperature, composition and flow rate or space velocity on the conversion of carbon dioxide to methane was determined. In view of the potential significance of the methanation reaction with the variation of different parameters in fluidized bed reactor rather than fixed bed, this study was undertaken.

CHAPTER-TWO

LITERATURE REVIEW

2.1 Fluidization

2.1.1 Introduction

A fluidized bed reactor is one in which relatively small particles of catalyst are suspended by the upward motion of a fluid. Virtually, in all industrial applicationS the fluid is a gas which flows upward through solid particles at a rate which is sufficient to lift them from a supporting grid, but which is not so large as to carry them out of the reactor or even to prevent them from falling back into the fluidized phase above its free surface. The particles are in constant motion within a relatively confined region of space, and extensive mixing occurs in both the radial and longitudinal direction of the bed (10).

Fluidized bed reactors were first employed on a large scale for the catalytic cracking of petroleum fractions, but they have since then been employed for an increasingly large variety of reactors, both catalytic and noncatalytic. The catalytic reactions includes the partial oxidation of naphthalene to phthalic anhydride and formation of acrylonitrile from propylene, ammonia and air. The noncatalytic applications include the roasting of ores and the fluorination of uranium oxide.

2.1.2 Conditions for Fluidization

Consider a vertical tube partly filled with a fine

granular material such as catalytic cracking catalyst. The tube is open at the top and has a porous plate at the bottom to support the bed of catalyst and to distribute the flow uniformly over the entire cross section. Air is admitted below the distributor plate at a low flow rate and passes upward through the bed without causing any particle motion. If the particles are quite small, flow in the channels between the particles will be laminar and the pressure drop across the bed will be proportional to the superficial velocity (V_0). As the velocity is gradually increased, the pressure drop increases, but the particles do not move and the bed height remains the same. At a certain velocity, the pressure drop across the bed counterbalances the force of gravity on the particles or the buoyant weight of the bed and any further increase in velocity causes the particles to move. This is point A on the graph (Fig. 2.1)

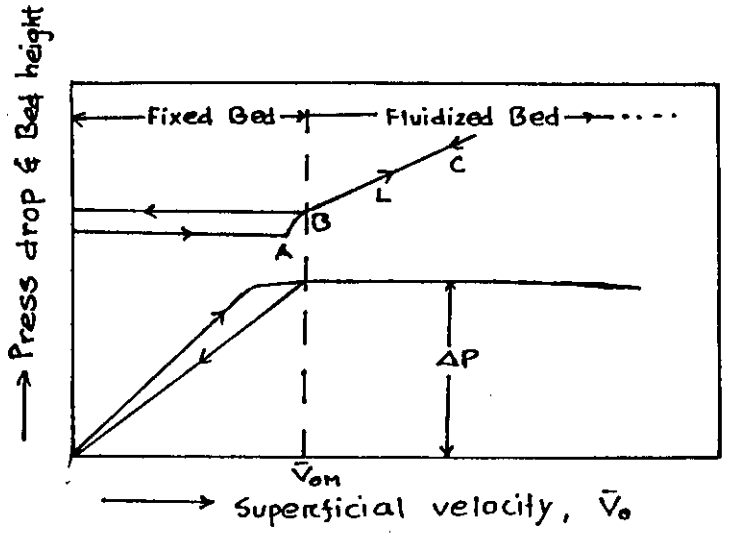

Fig. 2.1: Pressure and bed height vs. superficial velocity

Sometimes the bed expands slightly with the grains still in contact, since just a slight increase in voidage can offset an increase of several percent in superficial velocity. With a further increase in superficial velocity, the particles become separated enough to move about in the bed and true fluidization begins (Point B).

Once the bed is fluidized, the pressure drop across the bed stays constant, but the height continues to increase with increasing flow. If the flow rate to the fluidized bed is gradually reduced, the pressure drop remains constant, and the bed height decreases, following the line BC. However the final bed height may be greater than the initial value for the fixed bed, since solids dumped in a tube tend to pack more tightly than solids settling from a fluidized state. On starting up again, the pressure drop offsets the weight of the bed at point B, and this point, rather than point A, should be considered to give the minimum fluidization velocity, V_0 .

2.1.3 Minimum Fluidization Velocity:

An equation for the minimum fluidization velocity relating particle size, porosity and the density of fluid of fluid particle are given by:

$$\bar{V}_{oM} \approx \frac{\Phi_s^2 D_p^2 g(\rho_p - \rho)}{150\mu} \frac{\epsilon_M^3}{1-\epsilon_M} \qquad (2.1)$$

Again the terminal settling velocity to the laminar region is given by (12):

$$u_t = \frac{gD_p^2 (\rho_p - \rho)}{18\mu} \qquad (2.2)$$

The ratio $u_t/\bar{V}_{oM}$ gives

$$\frac{U_t}{\bar{V}_{OM}} = \frac{8.33(1-\epsilon_M)}{\phi_s^2 \epsilon_M^3} \qquad (2.3)$$

So the ratio $u_t/\bar{V}_{oM}$ depends mainly on the void fraction at minimum fluidization. For spheres, with $\epsilon_M \simeq 0.45$, the terminal settling velocity is 50 times the minimum fluidization velocity. For nonspherical particles, ϕ_s it is less than 1. However, the value of ϵ_M is generally greater for irregular particles than for spheres, and for $\phi_s = 0.8$ and $\epsilon_M = 0.5$, the ratio $u_t/\bar{V}_{oM}$ is 52, about the same as that estimated for spheres.

2.1.4 Types of Fluidization:

2.1.4.1 Bubbling Fluidization

Beds of solids fluidized by air usually exhibit what is called aggregative or bubbling fluidization. At superficial velocity much greater than $\bar{V}_{oM}$ most of the gas passes through the bed as bubbles or voids which are almost free of solids, and only a small fraction of the gas flows in the channels between the particles. the particles move erratically and are supported by the fluid, but in the space between bubbles, the void fraction is about the same as at incipient fluidization. The behavior of a bubbling fluidized bed depends very strongly on the number and size of the

gas bubbles, which are often hard to predict. The average bubble size depends on the nature and size distribution of the particles, the type of distributor plate, the superficial velocity and the depth of the bed.

2.1.4.2 Particulate Fluidization

When the fluidizing fluid is liquid, beyond the minimum fluidization velocity $\bar{V}_{oM}$, the particles move further apart and their motion becomes more vigorous as the velocity is increased, but the average bed density at a given velocity is the same in all sections of the bed. this is called particulate fluidization and is characterized by a large but uniform expansion of the bed at high velocities.

The generalization that liquids give particulate fluidization while gases give bubbling fluidization is not completely valid. The density difference is an important parameter, and very heavy solids may exhibit bubbling fluidization with water, while gases at high pressure may give particulate fluidization of fine solids. Also, fine solids of moderate density, such as cracking catalysts, may exhibit particulate fluidization for a limited range of velocities and then bubbling fluidization at high velocities.

2.1.4.3 Slugging Fluidization

If a small diameter is used with a deep bed of solids, the bubbles may grow until they fill the entire cross section.

Successive bubbles then travel up the column separated by slugs of solids. A situation is reached where the vessel dimensions determine the bubble size, which is called slugging regime or slugging fluidization. An advantage of slugging in reactors is that the slugs have a well defined shape, are easy to observe, and reliable reactor models can be made based on many investigations.

2.1.4.4 Turbulent Fluidization

At higher velocities slugging beds or bubbling beds may disintegrate, and a turbulent structure may occur in which dense and less dense domains or streaks are visible, which can hardly be called bubbles and dense phase. This regime is called turbulent fluidization. The transition to this regime is not well defined, but for cracking catalysts the transition from bubbling bed to turbulent bed will roughly occur at a velocity between 0.4 and 0.8 m/s, depending on the particle size.

2.1.5 Modeling of Fluidization:

A number of different types of reaction are commonly carried out in fluidized reactors; gas phase reactions, solid-catalyzed reactions, and reactions involving reaction between gas and solid phases. Catalytic reactions are probably the most common in chemical engineering, but in all these cases, and particularly the last two, what is important is the contact time distribution between the two phases. For heterogeneous reaction the contact time distribution plays the same role as the residence time distribution for homogeneous reactions. Practically the behaviour of a bed

depends strongly on many variables: particles, gas flow, bed diameter, distributor design etc.

In two phase system, the presence of bubbles, and their effect on gas/solid contacting and mixing, lies at the root of the bed's behaviour. May's model (11), described the bubbling bed as a two phase system, characterized by an interchange between the bubbles and the emulsion or dense phase (Fig. 2.2). The bubble phase, which is free of particles, is essentially in plug flow and the gas mixing in the dense phase is characterized by a dispersion coefficient. It is worth noting that May's model gives a reasonable account of the effects of gas interchange on reactor performance.

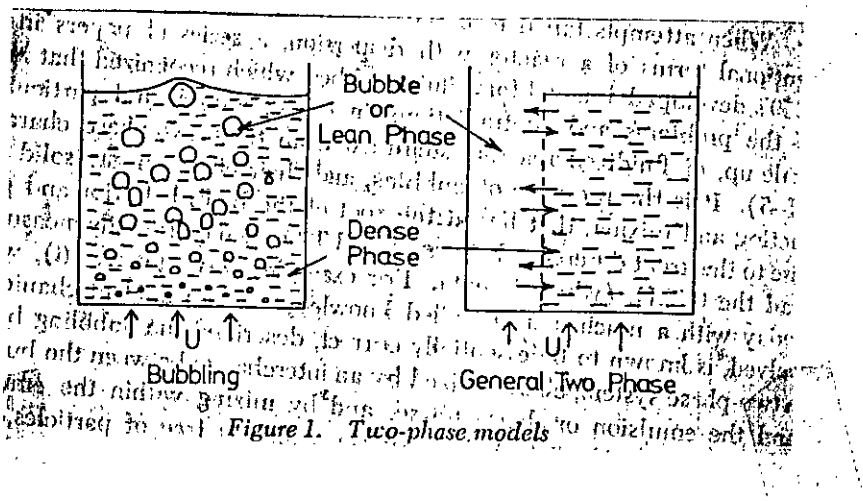

Figure 1. Two-phase models

Fig. 2.2: Two phase model.

Orcutt, Davidson and Pigford (11) developed a model relating bubble rising velocity, bubble size and with gas velocity. In this theory

the bubble rising velocity is considered proportional to the square root of the bubble radius, which is consistent with the assumption that the particles move around the essentially spherical bubbles like an inviscid liquid. Davidson's model also accounted the resistance to diffusion within the particulate phase for the interaction between the convective flow. He determined the significance interchange depends on $\alpha = U_b/U_0$ which is the ratio between the bubble velocity and the interstitial gas velocity at incipient fluidization. As Davidson showed, and subsequent experiments have confirmed, the gas flow relative to a rising bubble depends strongly on α (Fig. 2.3).

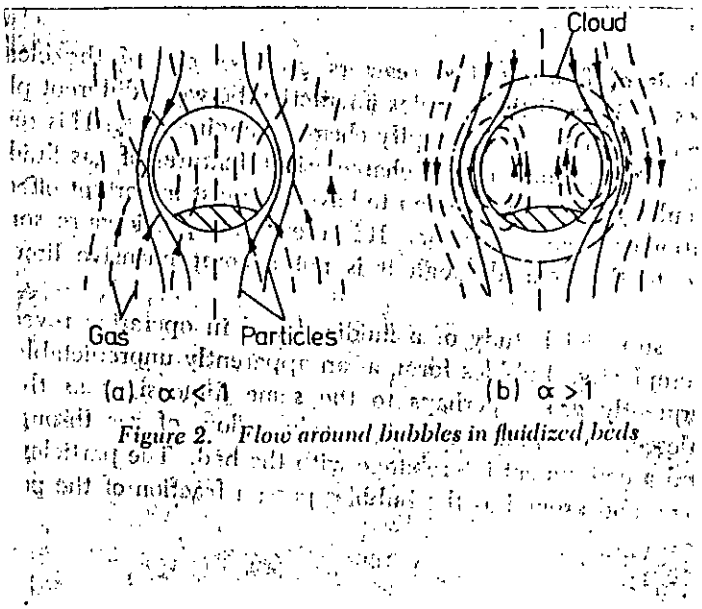

Fig. 2.3: Flow around bubbles in fluidized bed.

Rowe and Partridge's (11) assumed that the bubble plus cloud ensemble is perfectly mixed and that a fraction of the gas within

this ensemble, equivalent to the volume of the surrounding cloud and wake, is in contact with the particles at any instant. The significance of this assumption can be grasped by the analogy shown in Fig. 2.4. The equation which describes the situation are:

$$d/dt\ (V_1C_1 + V_2C_2) = -k_vV_1C_1 \qquad (2.4)$$

where,

V_1, V_2 : Volumes of bubble cloud and void.

C_1, C_2 : Concentration in cloud and in void

K : rate constant

The assumption implicit in Rowe and Partridge's model is that the time constant ($=V_2/Q$) of the empty bubble is much smaller than that of the cloud and wake where the reaction is proceeding. Since in general $V_1<V_2$, This could only be exactly true if interchange were infinitely fast although in practice with slow reactions the assumption will be more nearly correct.

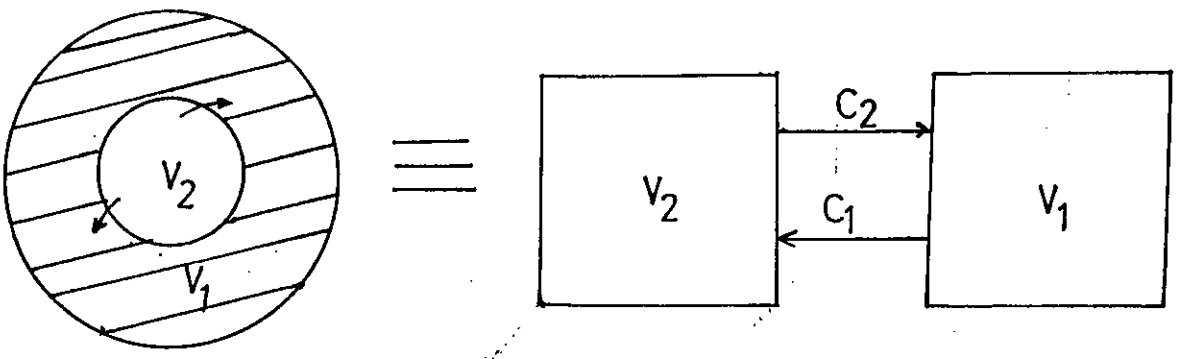

Fig. 2.4: Reaction in bubble cloud.

2.1.6 Advantages in using fluidized bed reactors

Several advantages are associated with the use of fluidized bed reactors. Uniform temperature can be maintained throughout the catalyst bed. This property is a consequence of the high degree of turbulence within the bed, the high heat capacity of the solid catalyst comprising the bed relative to the gas contained therein, and the extremely high interfacial area for heat transfer between the solid and the gas phase. These facilitate control over the temperature of the reactor and its contents. This in turn enhances the selectivity that can be achieved and permits very large scale operation.

The advantage of fluidized bed reactors is that they permit continuous, automatically controlled operations using reactant catalyst systems that requires catalyst regeneration at very frequent intervals. Fluidized bed operation permits one to easily add or remove the catalyst from the reactor or the regenerator. Regeneration can be achieved by any convenient procedure, but the use of fluidized bed regeneration permits continuous operation and is usually most economical. Furthermore, the circulation of solids between two fluidized beds makes it possible to transfer large quantities of energy between the reactor and the regenerator. The feature is particularly useful in catalytic cracking reactions where the exothermic regeneration reaction can be used thereby to supply some of the energy requirements for the endothermic cracking reactions.

2.1.7 Disadvantages in using fluidized bed reactor

Disadvantages are also associated with fluidized bed reactors. They cannot be used with catalyst solids that will not flow freely or that have a tendency to agglomerate. Attrition of the solids also causes some loss of materials as fines, which are blown out of the reactor. Extensive solids collection systems including cyclone separators and electrostatic precipitation must often be provided to minimize catalyst losses and contamination of the environment. Another disadvantage of the fluidized bed operation is that it leads to a larger pressure drop than fixed bed operation. Erosion of pipes and reactor internals by particles can occur. In general, operating and maintenance cost will be relatively high for this mode of operation compared with similar scale operations with other reactor types. Fluidized bed operations also have the disadvantage that the fluid flow deviates markedly from plug flow, and the bypassing of solids by bubbles can lead to inefficient contacting. This problem is particularly significant when dealing with systems in which high conversions are desired. It can be circumvented to some extent by using multiple beds in series.

2.2 Methanation of carbon dioxide:

2.2.1 Thermodynamics

The principal reaction which occur during methanation of CO_2 is

$$CO_2 + 4H_2 \longrightarrow CH_4 + H_2O \qquad (2.5)$$

This is a highly exothermic reaction. It has a heat of reaction of -39.5 KCal/gmol (Table-2) at 298°K. Equilibrium constant for this reaction may be defined by

$$K_{pCO2} = \frac{P_{CH4}\, P^2_{H2}O}{P_{CO2}\, P^4_{H2}} \qquad (2.6)$$

The value of equilibrium constant decreases with increasing temperatures. Table 2.1 shows equilibrium constants for CO_2 methanation at different temperatures. The exothermic nature of the methanation reaction gives a temperature rise corresponding to a given conversion of CO_2. The temperature rise for a typical methanator gas composition (CO .5%, CO_2, .2%, H_2O, 1%, $H_2$73.3%, CH_4 1%, N_2 24%) is 60°C per 1% of CO_2 converted. Specific heats for different components of the gas streams vary with temperature but are independent of pressure. Table 2.2. lists specific heats and heats of formation of the various components of the gas streams, catalysts, supports, etc.

Table 2.1 $K_{p,CO2}$ Values at different temperatures

Temperature(°C)	Equilibrium Constant (atm^{-2})
200	$.94748X10^{9}$
220	$.15589X10^{9}$
240	$.29435x10^{8}$
260	$.62706x10^{7}$

280	$.14863 \times 10^{7}$
300	$.38747 \times 10^{6}$
320	$.11001 \times 10^{6}$
340	$.33737 \times 10^{5}$
360	$.11094 \times 10^{5}$
380	$.38882 \times 10^{4}$
400	$.14442 \times 10^{4}$
420	$.56582 \times 10^{3}$
440	$.23282 \times 10^{3}$
460	$.10023 \times 10^{3}$
480	$.44995 \times 10^{2}$
500	$.20997 \times 10^{2}$
520	$.10157 \times 10^{2}$
540	$.50814 \times 10^{1}$
560	$.26225 \times 10^{1}$
580	$.13936 \times 10^{1}$
600	$.76104 \times 10^{1}$

Table 2.2 Thermodynamic data relevant to CO_2 methanation

Specific heats:

(a) Catalyst:

NiO : $C_p = 11.3 + 0.00215T$ Cal/deg. $^{0}C.gmol.$

Ni : $C_p = 4.26 + 0.0064T$ "

Al_2O_3 : $C_p = 22.08 + 0.008971T - 522500T^{-2}$ "

(b) Gas streams:

H_2 : $\bar{C}_p = 6.62 + 0.0081T$ Cal/gmol ^oC

N_2 : $\bar{C}_p = 6.5 + 0.001T$ "

CO : $\bar{C}_p = 6.6 + 0.0012T$ "

CO_2 : $\bar{C}_p = 10.34 + 0.00274T - 1955T^{-2}$ "

CH_4 : $\bar{C}_p = 5.34 + 0.0015T$ "

H_2O : $\bar{C}_p = 8.22 + 0.000157T - 0.00000134T^2$ "

Heats of formation:

NiO : $\Delta H_f^{298} = -58.4$ Kcal/gmol

H_2O : $\Delta H_f^{298} = -57.7979$ "

CO : $\Delta H_f^{298} = -26.416$ "

CO_2 : $\Delta H_f^{298} = -94.052$ "

CH_4 : $\Delta H_f^{298} = -17.889$ "

Heats of reaction:

$CO_2 + 4H_2 \rightarrow CH_4 + 2H_2O$ $\quad \Delta H_r^{298} = -39.5$

$NiO + H_2 \rightarrow Ni + H_2O$ $\quad \Delta H_r^{298} = 0.61$

$Ni + 1/2\ O_2 \rightarrow NiO$ $\quad \Delta H_r^{298} = -58.4$

2.2.2 Kinetics:

Methanation of CO_2 is first order with respect to CO_2 when the concentration of CO_2 is sufficiently low such as the concentration in CO_2 scrubber effluent. Under these conditions the reaction kinetics has been proposed (7) in the following manner.

Methanation reaction:

$$CO_2 + 4H_2 = CH4 + 2H_2O \qquad (2.7)$$

Assuming pseudo first order reaction on carbon dioxide, the rate of reaction may be expressed as follows:

$$r = k\,(C_R - C_p/K) \qquad (2.8)$$

Substituting $C_p = x_R$, $C_R = 1-x_R$

$$\text{and } K = \frac{x_{eq.R}}{1 - x_{eq.R}}$$

Equation (2.8) may be changed as follows:

$$r = k\left(1 - \frac{x_R}{x_{q.R}}\right) \qquad (2.9)$$

where r : rate of reaction.

k : rate constant, k is the Arrhenius form function of temperature.

C_R : mols of reactant

C_p : mols of product

K : equilibrium constant.

On the other hand, from the mass balance over catalytic unit, the following equation may be obtained.

$$F.\,dx_R = r\,dW \qquad (2.10)$$

where, F : feed rate, mass per unit time.

W : mass of catalyst in reactor.

r : reaction rate, mols/mass of catalyst/time

x_R : conversion, mols/unit mass of feed.

By integrating equation (2.9), equation (2.10) can be obtained,

$$\frac{W}{F} = \frac{1}{SV_w} = \int_0^{x_R} \frac{dx_R}{r} \qquad (2.11)$$

where SV_w: space velocity, volume of feed/vol. of cat./unit time

From equation (2.9) and (2.11), equation (2.12) may be derived.

$$k = x_{eq.R}\, SV_w \ln\left(\frac{1}{1 - \frac{x_R}{x_{eq.R}}}\right) \qquad (2.12)$$

Since $x_{eq.R}$ is constant under given conditions,

$$K_w = SV_w \log\left(1 - \frac{1}{\frac{x_R}{x_{eq.R}}}\right) \qquad (2.13)$$

Since reactant R is CO_2 here,

$$x_R = x_{CO2} = \frac{CO_2,\ in - CO_2,\ out}{CO_2,\ in}$$

$$x_{eq.CO_2} = \frac{CO_2,\ in - CO_2\ eq.\ out}{CO_2,\ in}$$

where CO_2, in : mols of CO_2 inlet.

CO_2, out: mols of CO_2 outlet

CO_2 eq. out: mols CO_2 outlet at equilibrium

Therefore equation (2.13) may be changed as follows:

$$K_w = SV_w \log \left(\frac{CO_2,\ in - CO_2,\ eq.\ out}{CO_2,out - CO_2\ eq.\ out}\right)$$

$$\text{Or, } K_w = SV \left(\frac{S}{G} + 1\right) \log \left(\frac{CO_{2,in} - CO_2.\ eq.\ out}{CO_2,\ out - CO_2.\ eq.\ out}\right)$$

where; SV : dry gas space velocity at inlet condition

SV_w : $SV(S/G + 1)$

S/G : Steam to dry gas mol ratio, inlet basis.

$$\text{Or, } SV = \frac{Kw}{\left(\frac{S}{G} + 1\right) \log \left(\frac{CO_2,in - CO_2.\ eq.\ out}{CO_2,out - CO_2,\ eq.out}\right)} \qquad (2.14)$$

Actually, rate constant k (consequently K_w) is determined by various factors such as temperature, operating pressure, catalyst size factor, catalyst aging factor etc.

2.2.3 Mechanism

Two proposed schemes for the mechanism of synthesis of methane from carbon dioxide and hydrogen have been discussed by Mills & Steffgen (5). According to one scheme the reduction of CO_2 to CH_4 occurs with the intermediate formation of CO.

The other scheme suggests that the reaction does not proceed through intermediate CO formation.

The idea that CO_2 does not react by a mechanism not involving

intermediate CO formation was proposed as the following reaction sequence.

$$CO_2 \xrightarrow{+2H_2} H_2-C(OH)(OH) \xrightarrow{-H_2O} CH_2O \xrightarrow{+H_2} CH_3OH \xrightarrow{-H_2O} CH_2 \xrightarrow{+H_2} CH_4 \qquad (2.15)$$

In addition to the direct methanation of CO_2, there is evidence that CO_2 is removed by the water gas shift reaction(9), by conversion to CO;

$$CO_2 + H_2 \longrightarrow CO + H_2O \qquad (2.16)$$

If a catalyst is tested with CO_2, with no CO in the inlet gas, a trace of CO is found, indicating the occurrence of the above reaction.

Later the mechanism for hydrogenation of CO_2 have been reviewed by Yuzefovich et. al (8) in detail. They conclude that kinetic data cannot confirm a particular mechanism directly and that evidence by independent methods is required.

They found from weighing experiments that there is no significant adsorption of CO_2 and the products of its transformation. Further, when they introduced a mix of H_2 and CO_2 to the untreated catalyst, the work function remained unchanged relative to that in an atmosphere of hydrogen. This indicates that adsorption of CO_2 and the formation of complexes influencing the electronic structure of the catalyst does not take place on the surface of the catalyst containing dissolved hydrogen. They

adsorption of CO_2 and the formation of complexes influencing the electronic structure of the catalyst does not take place on the surface of the catalyst containing dissolved hydrogen. They conclude that recent experimental results refute the suggestion that the start of formation of CH_4 from CO_2 on nickel catalysts is preceded by the adsorption of both components of the reactions, and indicate that hydrogen adsorbed on the catalyst surface reacts with molecules of carbon dioxide in the gas phase.

Vlasenk and Yuzefovich (8) proposed another type of mechanism. They proposed that the formation of CH_4 from CO_2 and H_2 appears to be one in which the formation of complexes of a type corresponding to the enrol form of formaldehyde takes place initially, and in which the subsequent transformations are analogous to the stages in the hydrogenation of CO, but with the significant difference that in the reduction of CO_2 these changes take place not on the catalyst surface, but in the volume of the gas -

The mechanism proposed (8) is

$$2[\ \ ] + 2e + H_2 \longrightarrow 2[H]^-$$

$$2[H]^- + CO_2 \longrightarrow [HCOOH] \longrightarrow 2[\ \ ] + C(OH)_2 + 2e(slou)$$

$$C(OH)_2 + H_2 \longrightarrow HCOH + H_2O$$

$$H - C - OH + H_2 \longrightarrow CH_2 + H_2O$$

$$CH_2 + H_2 \longrightarrow CH_4$$

According to this scheme, the process is initiated by the activation of only the hydrogen on the catalyst surface, after which the reaction takes place in the gas volume.

2.2.4 Catalysts

2.2.4.1 Overview

Early in the 1920s Fischer, Tropsch, and Dilthey (8) compared the methanation properties of various metals at temperatures upto 800°C. The decreasing order of methanation activity was Ru, Ir, Rh, Ni, Co, O_s, P_t, Fe, Mo, Pd, Ag. Thus by 1925 all of the metals now considered active for methanation of carbon oxides had been identified. In terms of metals important for methanation, the list could now be shortened to Ru, Ni, Co, Fe and Mo.

Further progress over the past 50 years has had to do with preferred promoters, supporters, and preparation conditions to obtain high selectivity and to maintain catalytic activity. A brief description of pertinent literature since the mid 50's follows in which the catalysts are grouped according to their most active constituent.

2.2.4.2 Nickel

As a methanation catalyst, nickel is preeminent; the metal is relatively cheap, it is very active when present in a form having high surface area, and it is the most selective to methane of all materials.

Alloys of nickel with different proportions of copper is found to vary in their selectivity when methanating CO_2. Good selectivity to methane is achieved only with pure nickel and selectivity to CO is very pronounced with greater than 4% copper in the alloy; with more than 50% copper, amount of CO obtained is high, but with no methane. The conversion of CO_2 remains unchanged for alloys ranging from 4 to 100% copper as shown in Fig. 2.4A.

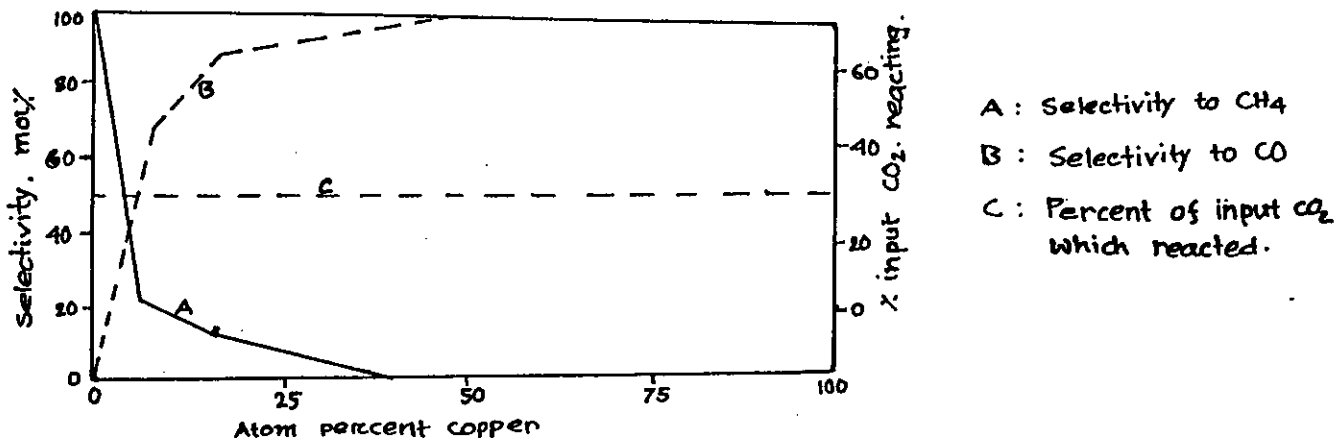

Fig. 2.4A: Hydrogenation of CO_2 over nickel-copper catalysts

The main drawback of the nickel catalyst is that it is easily poisoned by sulfur compounds, a fault common to all of the highly active methanation catalysts. Sulfur can poison a methanation catalyst permanently and drastically reduce its activity. In fact, a given amount of sulfur may possibly poison a methanation catalyst more severely than it does a reforming catalyst (7). It is also true that nickel can react with CO to form a carbonyl $Ni(CO)_4$, a carbide Ni_3C or even free carbon but these are

easily avoided through the proper selection of reaction temp. and use of an excess of H_2 over the stoichiometric ratio.

2.2.4.3 Ruthenium

Ruthenium was early recognised as a very active methanation catalyst. Though its cost is very high, this catalyst can compete with cheaper catalysts for long catalytic life and high activity and selectivity. Traces of sulfur compounds rapidly deactivate the ruthenium catalyst.

With this catalyst at atmospheric pressure and at 300°C the methanation reaction gives only methane (5). At higher pressure the reaction initiates at lower temperature but higher molecular weight products with increasing pressure. A catalyst containing 0.5 wt% ruthenium at 250°C using various H_2/CO_2 and H_2/CO ratio, low ratios invariably give large amounts of high molecular weight products while relatively more methane form with a higher ratio; also lower pressure favours methane production.

2.2.4.4 Cobalt and Iron

In 1956 the British Bureau of Mines investigated catalysts derived from Raney alloys as a means of synthesis of high Btu fuel gas (8). Raney cobalt, when extracted with alkali to remove a portion of aluminum, was found to be very active for methanation, producing gas with a CO_2 free heating value over 950 Btu/CF at high space velocity. However, that catalyst tended to deposit carbon more than nickel catalysts under the same operating conditions.

An unusual iron catalyst, carbon expanded iron, was discovered by the Bureau of Mines to have activity as a methanation catalyst. Iron catalyst, from steel turnings that were first oxidized 20% in steam and then reduced, was used to methanate a 3:1 synthesis gas at 400 psig & 320°C using hot gas recycle. It is a very active form of iron and maintains its activity well, but ultimately carbon deposition leads to bridging and plugging of the reactor.

2.2.4.5 Molybdenum and Tungsten

Molybdenum and tungsten methanation catalysts stand out because they are sulfur resistant and, in fact, are commonly sulfided before use. A variety of molybdenum catalysts were prepared and tested for methanation activity by the Bureau of Mines at 21 atm and about 300 GPSU (11). Only moderately active catalysts were formed at best, and relatively high temperatures were required. The highest selectivity to CH_4 was 79 to 94%, obtained with a coprecipitated and sulfided catalyst.

A tungsten-alumina catalyst prepared by coprecipitation is quite inactive and requires 600°C for 43.6% conversion of 1:1 synthesis gas. Tungsten sulfide, WS_2, is more active in the direct methanation of CO or CO_2 present in the gasification product from coal to obtain a higher Btu fuel gas.

2.2.4.6 Industrial applications

At present, methanation is used to convert relatively small amounts of harmful carbon oxide to methane whereas in ammonia synthesis, carbon monoxide especially would interfere with catalytic utilization. Variations in the preparation, of nickel catalysts supported on alumina can greatly affect the activity and stability of the catalysts. The several types of catalysts are formulated on specifically prepared alumina supports which impart the optimum combination of catalyst activity and thermal stability (7). Although high activity is a basic requirement for the methanation catalysts, the support base must be able to withstand overheating without significant loss of catalytic properties. Catalysts prepared by impregnation of alumina with nickel nitrate had low activity and stability compared to a coprecipitated catalyst from nickel nitrate and sodium aluminate.

Cromia supported nickel catalysts varies with their different composition. With this variation, reduction time and temperature differs markedly. Ni-Cr_2O_3 catalysts are less active than nickel on kieselguhr or a coprecipitated catalyst from water glass and nickel nitrate. Nickel supported on kieselguhr has been widely used for a long time.

From an industrial viewpoint, high selectivity to methane is not difficult to achieve. Rather the problems are prevention of catalyst deactivation by sulfur compounds or carbon deposition and also those arising from the highly exothermic nature of methanation.

With nickel catalysts it is usual to limit sulfur in the gas to less than 1 ppm by providing rigorous purification. Carbon deposition on the catalyst can be avoided by operation with a significantly high hydrogen to carbon-oxides ratio. Excessive temperature in methanation are avoided by either limiting the carbon-oxides content of reactant gases or providing apparatus to permit heat removal.

2.3 Previous work

Methanation, the hydrogenation of carbon oxides to methane, has been the subject of a large number of catalytic studies during the past 70 years. Study of methanation of CO_2 in fluidized bed reactor have rarely been done. However, there are several studies of the general aspects of this reaction in other reactors. These are reviewed in this section as some aspects of these studies are quite relevant to the present work.

W. Debruijn and et. al. (1) studied the methanation of carbon dioxide in hydrogen at atmospheric pressure in a parallel passage reactor. The rate equation for the methanation reaction they proposed is

$$r_{CO2} = \frac{K_{\alpha} \exp(-E_a/RT) P_{CO2}}{1+K_{CO2} P_{CO2}} \qquad (2.17)$$

They assumed mass transport in channel screen and catalyst bed entirely due to diffusion. On the basis of that assumption, they developed a model relating concentration as

$$D_{eff}\left(\frac{\partial c}{\partial y}\right)_{y=y_k} = D_{eff}\ \{\ -\frac{2A}{B^2}\ (BC_k - \ln(1+BC_k))\}^{1/2} \qquad (2.18)$$

where,

A = $\rho_{bed}\ K_{\alpha}\ RT\ \exp(-Ea/RT)\ Deff.$

B = $K_{CO2}\ RT$

C_2 = Conc. in catalyst bed at wire screen

C = Concentration

Y = Running variable perpendicular to direction off flou.

Y_k = Y, behind wire screen.

Van Herwijneu et. al (6) studied methanation of CO and CO_2 on a nickel catalyst in tubular reactor. They assumed the localised Langmuir chemisorption which leads to kinetic equation known as Langmuir Hinshelwood kinetics, as Eley-Redial mechanisms and also as Hougen-Watson models. Following this approach, the general form of kinetic equation is

$$r = \frac{K\ \exp(-E/RT).g(P).(1-\beta)}{1 + f(P,T)^m} \qquad (2.19)$$

In this equation g(P) is a pure kinetic term which is followed by a correction for the deviation from thermodynamic equilibrium, $(1-\beta)$. In the denominator, f(P,T) originates from the coverage balance over the active sites and m is the number of sites involved in the rate determining step.

Their approach was that the value of β is very small so that it can be neglected, g(p) is only a function of the partial

pressure of hydrogen and the carbon oxides, provided that the effects of the reaction products in the numerator used not be taken into account. Furthermore, they considered, partial pressure of hydrogen is very large compared to that of the carbon oxides and as a consequence g(p) is a function of carbon oxides only. For the same reason the contribution of hydrogen to the denominator can be neglected. They supposed that dissociative adsorption of CO, CO_2, CH_4 or H_2O does not occur, which resulted in a simplified rate equation:

$$r_{CO2} = \frac{K_{\alpha} \exp(-E/RT)\ P_{CO2}}{(1+K_{CO2}\ P_{CO2} + K_{H2O}P_{H2O} + K_{CH4}P_{CH4})^{n}} \qquad (2.20)$$

when reactants only are present, this equation becomes

$$r = \frac{K.\ P_{CO2}}{(1+K_{CO2}.P_{CO2})^{n}} \qquad (2.21)$$

Debruiju and et. al (1) studied the methanation reaction in the temperature range of 208-242°C and at atmospheric pressures. Volume flow rate and carbon dioxide concentration (vol%) in inlet was in the range 0.05-0.45 Nm^3/h and 0.19-2.56 vol% respectively. They used the methanation catalyst Girdler G.65 Ni/Al_2O_3; N_iO/Al_2O_3 = 3:3 w/w; particle size = 0.35-.42 mm.

The authors presented their experimental results graphically as conversion vs. space velocity for three temperature at several concentrations of CO_2 in hydrogen.

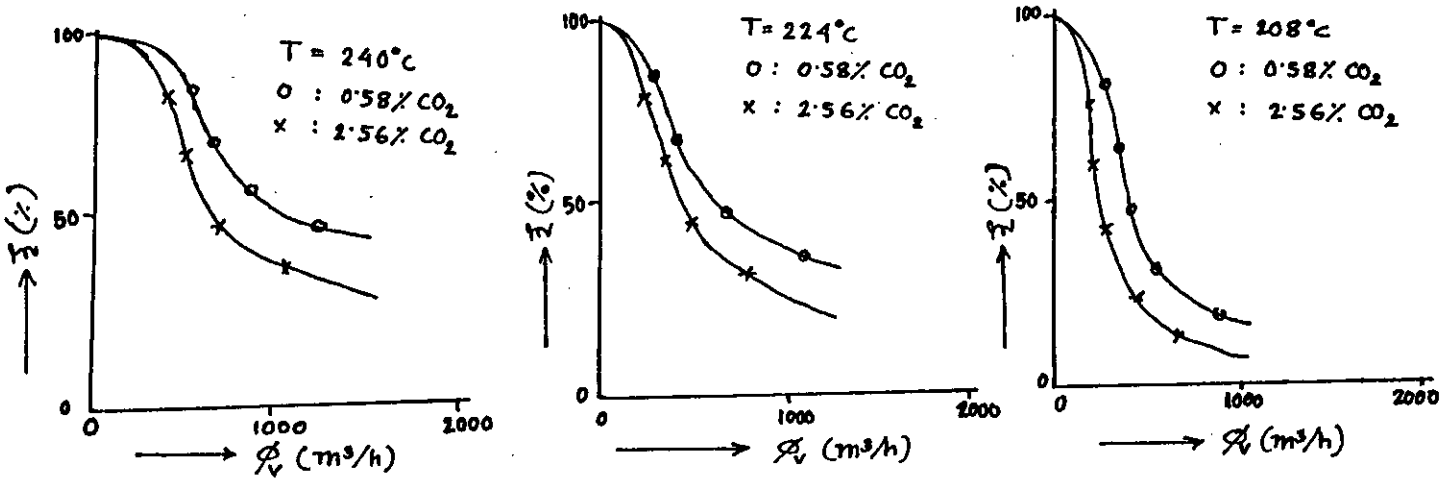

Fig. 2.4B: Plot of conversion against space velocity

They showed, at high space velocities, i.e. at low residence times, the ratio of mass transport through the channel into the catalyst is relatively high, resulting in low CO_2 conversion. As the flow rate of gas in the channel was decreased, the above ratio diminished and a larger proportion of CO_2 was converted. At very low space velocities the residence time apparently was long enough to give complete conversions.

Doesburg and Dejong (2) methanated CO_2 in a adiabatic fixed bed methanator containing Ni/Al_2O_3 catalyst. They studied the response of a 0.5 litre methanator changing the inlet conditions with 0.6-2.5 vol% CO_2 in hydrogen; 180-280°C inlet temperature, and space velocity 5.0-32.0 hr^{-1}. They used G-65 catalyst, 25 wt% N_i on

Al_2O_3, dp = 0.42 - 0.60 mm, particle density 2750 kg/m^3, and particle porocity 0.46.

They considered three types of disturbances in the feed of CO_2 in hydrogen separately:

i) They increased stepwise the concentration in the feed to an isothermal reactor. With the inlet temperature of 241°C, Cin = 0.8% CO_2, SV=17000 hr^{-1} and after 195 seconds, they monitored the temperatures at different position throughout the length of the reactor. They plotted temperature versus length of the reactor and obtained the axial temperature profile shown in fig: 2.5

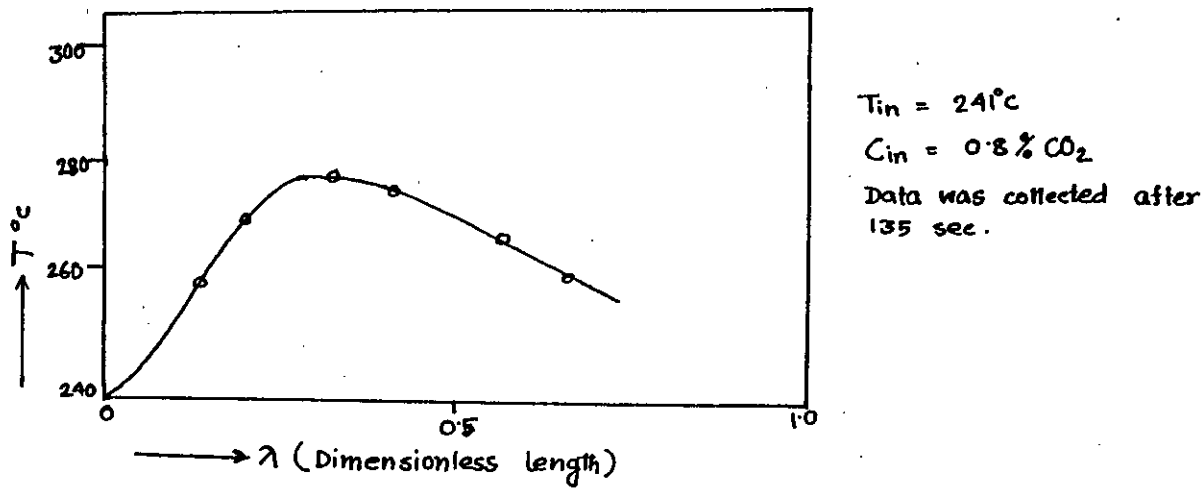

Fig. 2.5: Plot of temperature against dimensionless length of the reactor for data collection after 195 sec.

ii) In the next type, reactor was not isothermal. Insteads, there was an axial temperature profile at the time of the step change in concentration. They measured temperatures after 205 seconds throughout the length with change of inlet CO_2 concentration from Cin = 0.8% CO_2 to Cin = 1.72% CO_2 and same inlet temperature of 241°C, SV = 17000 hr^{-1}. The profile obtained is shown in Fig. 2.6.

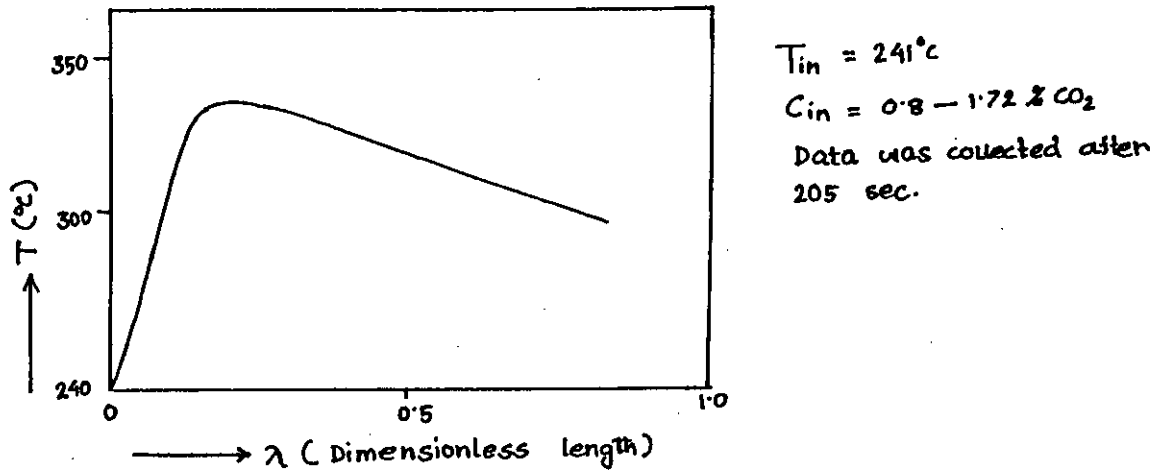

Fig. 2.6: Plot of temperature against dimensionless length of the reactor for collection of data after 205 sec.

In this type, they experimented the disturbance of feed temperature. They found, the temperature in the second part of the bed decreased when they increased entrance temperature; conversely, the temperature in the second part of the bed increased with decreasing feed temperature. They explained this by considering the lower conversion of CO_2 in the first part of the bed when the entrance temperature was low; more CO_2 reacted in the second part. That condition persists until the second part was cooled enough so that the exponential influence of the decrease in temperature overshadowed the competitive effect of the increased concentration on the reaction rate. A similar explanation applies to an increased feed temperature.

Herwijnen and et. al (6) used the nickel catalyst G-65. The

catalyst was of 36 wt% NiO and a BET surface area of 40 m^2/g; size of 0.35-0.42 mm. They measured the rate of hydrogenation of CO_2 at 200, 215 and 230°C in the concentration range 0.22 - 2.38% in hydrogen at a total pressure of 1 atm.

Firstly, they presented results graphically, the rate as a function of partial pressure of CO_2.

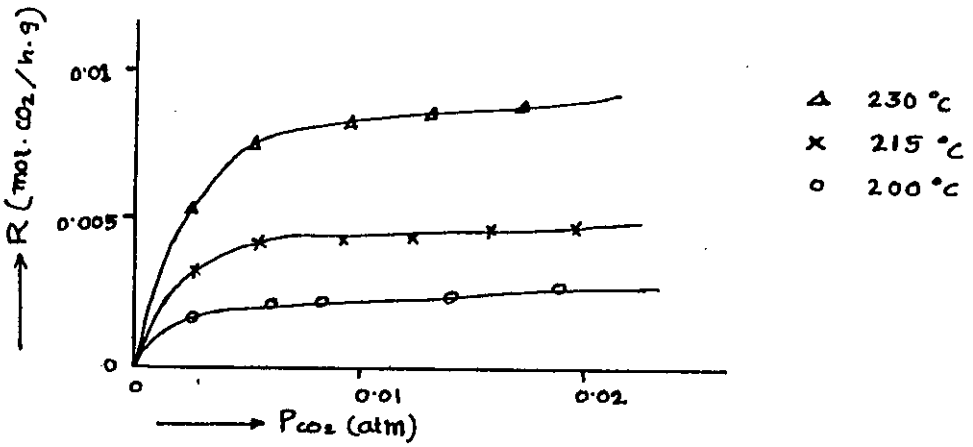

Fig. 2.7: Plot of rate as a function of partial pressure of carbon dioxide

They showed a change from first order dependency below 0.004 atm to zero order dependency at partial pressure above 0.015 atm. They described this with the langmuir isotherm, which meant that eqn. (2.21) holds with m equal to one. Transformation of that equation gives

$$\frac{1}{r} = \frac{1}{KP_{CO2}} + \frac{K_{CO2}}{k} \qquad (2.22)$$

To test the applicability of equation (2.22), they plotted 1/r as a function of $1/p_{CO2}$ at the three temperatures and obtained three straight line.

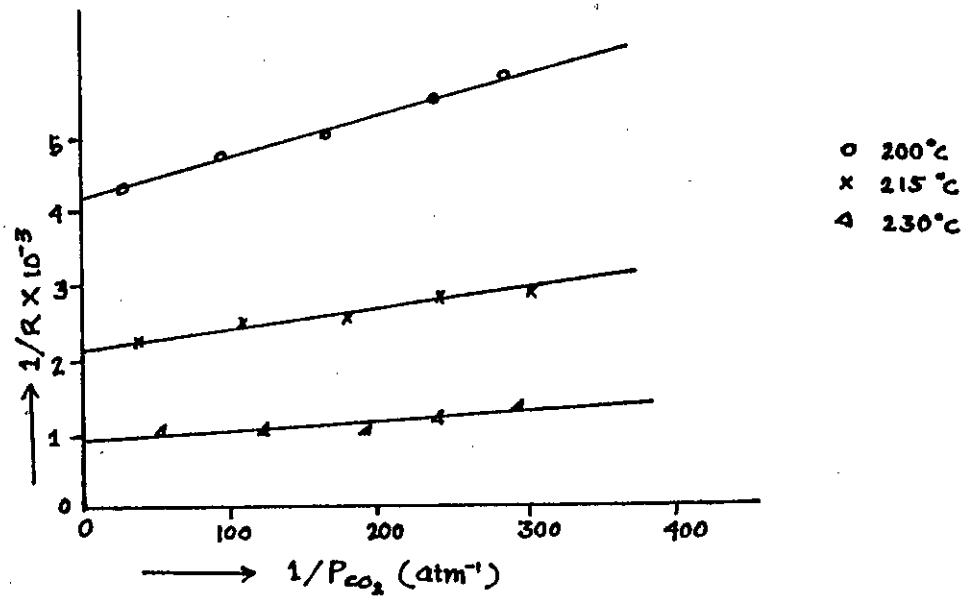

Fig. 2.8: Plot of reciprocal rate as a function of reciprocal practical pressure of carbon dioxide at different temperature.

Moreover they plotted conversion as a function of reciprocal space velocity at the three temperature. They found that conversion increases with increase of reciprocal space velocity i.e. conversion decreases with the increase of space velocity.

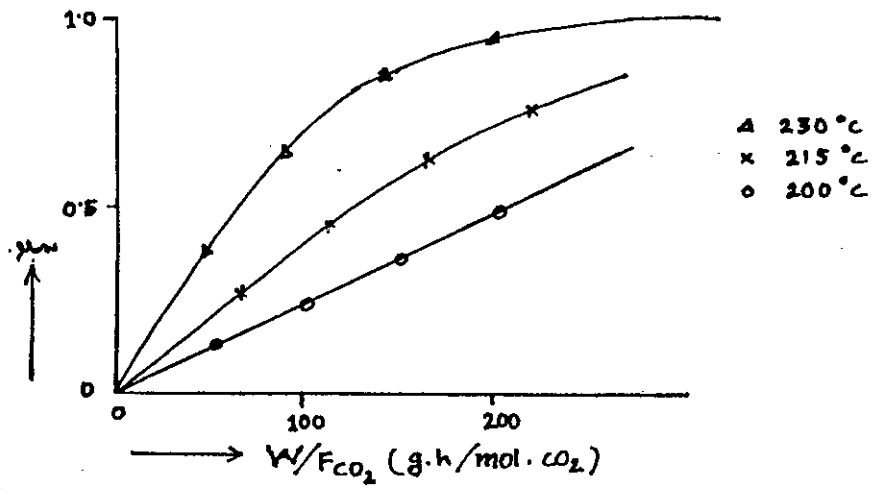

Fig. 2.9: Plot of conversion against reciprocal space velocity

They conclude that at higher reciprocal space velocities the residence time apparently was too high to give higher conversion rate.

Clang and Hopper (15) used nickel catalyst supported on Kieselguhr with a granule size 0.07-0.1mm. They investigated over a temperature range 276°C to 318°C and a total pressure from 155 to 250 psig. A range of space time from 0.03 to 0.2(h) (g of cat.)/ft^3 and a range of volume percent carbon dioxide in the feed from 17 to 33% they used.

The authors presented their experimental results plotting of conversion as a function of reciprocal space velocity for total pressures of 100, 155,200 and 250 psig with feed ratio H_2/CO_2 = 4:1. Similar plots for H_2/CO_2 of 2:1, 3:1, 4:1 and 5:1 with total pressure 250 psig were also presented.

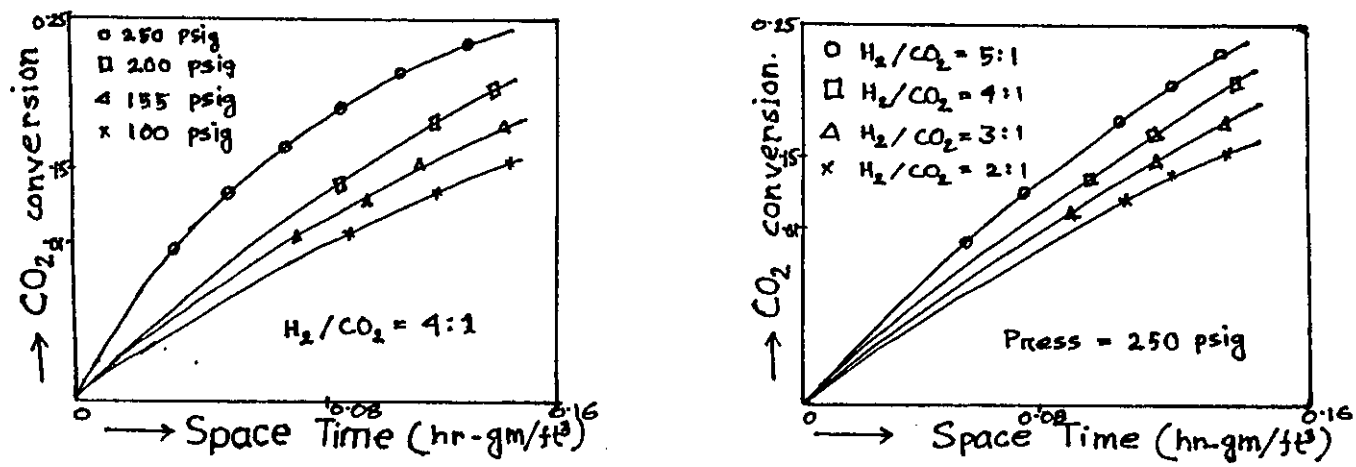

Fig.2.10:Plot of carbon dioxide conversion against space time.

They found that conversion of CO_2 increases with the space time for both cases. Their conclusion synchronized with that of Herwijnen and et. al (6) mentioned earlier.

J.N. Dew et. al(14) studied hydrogenation of carbon dioxide on nickel kieselguhr catalyst. They reduced the catalyst at a pressure of 30 atmosphere and a temperature of 320°C for 48 hours. They used a feed gas containing 20% CO_2 and 80% hydrogen and a pressure of 30 atmosphere to determine the effect of temperature on reaction rate. They increased the temperature incrementally starting from 193°C (380°F) until the maximum rate in methane formation had been covered. The temperature was then decreased incrementally to observe the thermal deactivation resulting from high temperatures. They presented the obtained results as a plot of reaction rate as catalyst temperature as shown in Fig. 2.11.

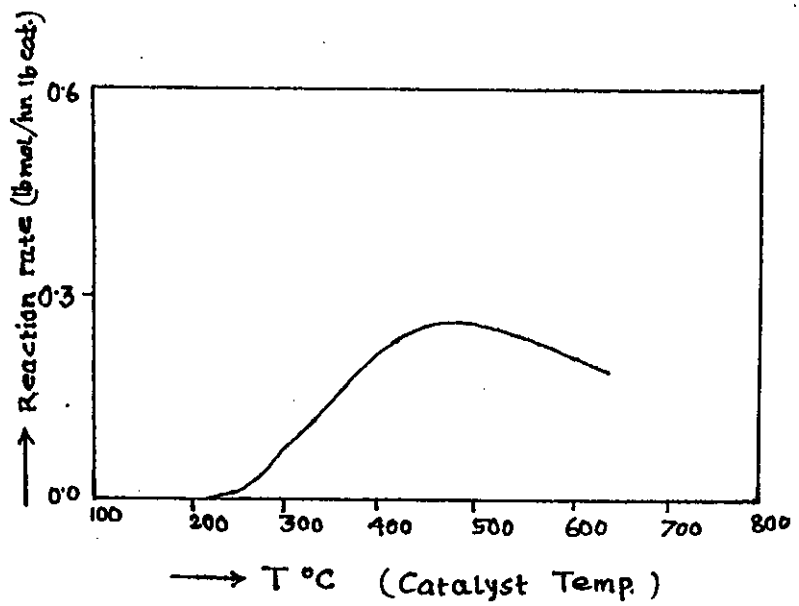

Fig. 2.11: Plot of reaction rate against catalyst temperature

They obtained a maximum reaction rate at 426°C (800°F) and this maximum reaction rate continued upto 515°C (950°F) and then decreased. During decreasing of temperature from a maximum of 665°C (1230°F) they observed that a threshold temperature does not exist. They conclude that the resistance to diffusion of the reactants into the catalyst pores consumes some of the driving potential for the over-all reaction. This resistance may become appreciable for small catalyst pores. The diameters of the catalyst pores decreased in size during exposure to higher temperatures. The effect of smaller pores on rate of reaction would be somewhat equivalent to the effect of lower total pressure since in either case the effective partial pressures of the reactants at the reaction sites would be lowered.

CHAPTER THREE

EXPERIMENTAL

3.1 Apparatus

3.1.1 Description of the experimental setup

The main part of the experimental setup is the reactor tube, which is divided into two sections. Between the two sections there are two mild steel distributor plates, one on top of the other. Each plate has a good number of 1 mm size holes. The holes are drilled in such a way that when the two plates are put in place, the holes in the two plates are staggered without any overlapping. Between the two distributor plates, a thin aluminum foil gasket is placed to allow the reacting gas mixture to flow from the lower plate to the upper plate. As a result of this arrangement adequate fluidization can occur in the reactor. The heating of the reactor is accomplished by use of a heating coil around the reactor. A thermocouple was introduced through a hole in the wall of the reactor tube just above the distributor plate. Temperature control was achieved by the help of a temperature controller connected to the heating coil.

The reactor top has been widened to arrest the catalyst particles which may get entrained in the gas stream. Catalyst was introduced into the reactor from the top through a hole which was kept closed during operation of the reactor. The fluid stream exits the reactor via a 0.25 inch diameter tube connected to the top of the reactor. A small 0.25 inch diameter tube was connected to

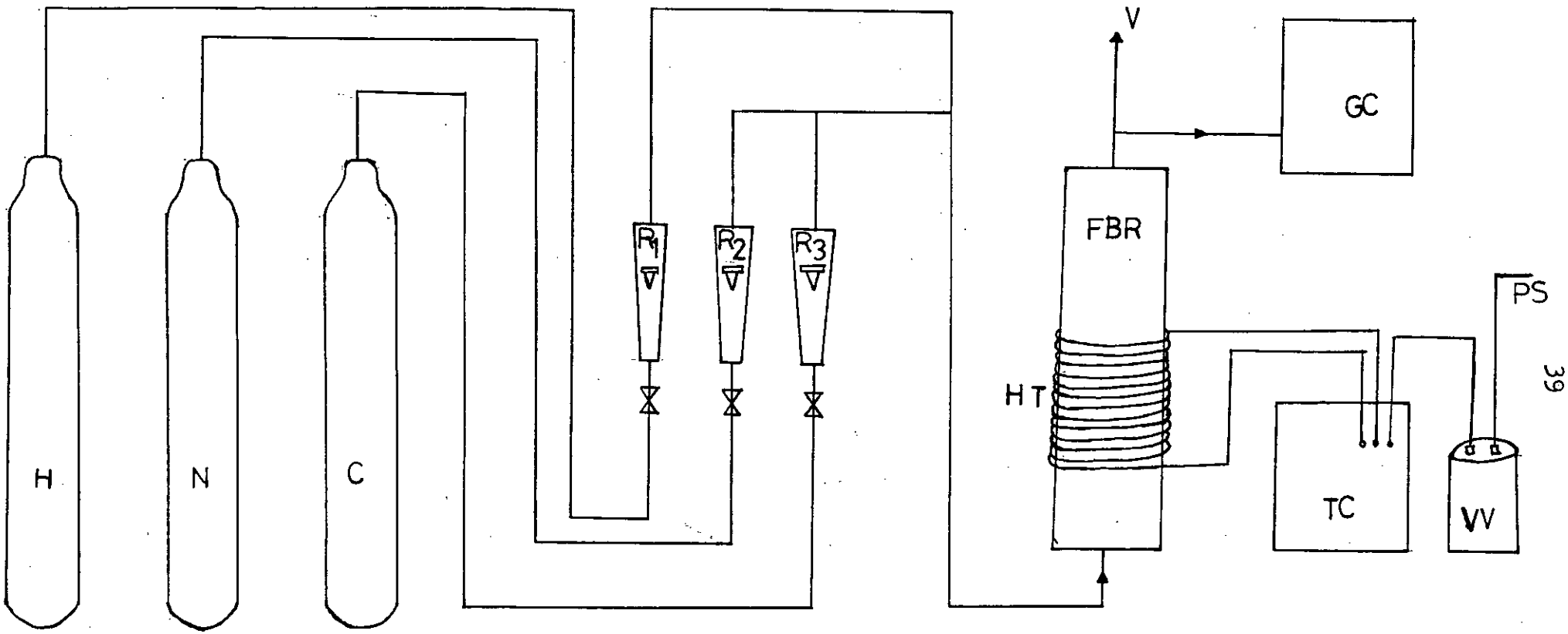

C : Carbon dioxide gas cylinder
H : Hydrogen Gas Cylinder
HT : Heating tape
FBR : Fluidized Bed Reactor
N : Nitrogen gas cylinder
PS : Power Source

R_1, R_2, R_3 : Rotameters
TC : Temperature Controller
V : Vent Line
VV : Voltage Variac

Fig. 3.1: Schematic Diagram of a Fluidized-Bed Reactor Assembly.

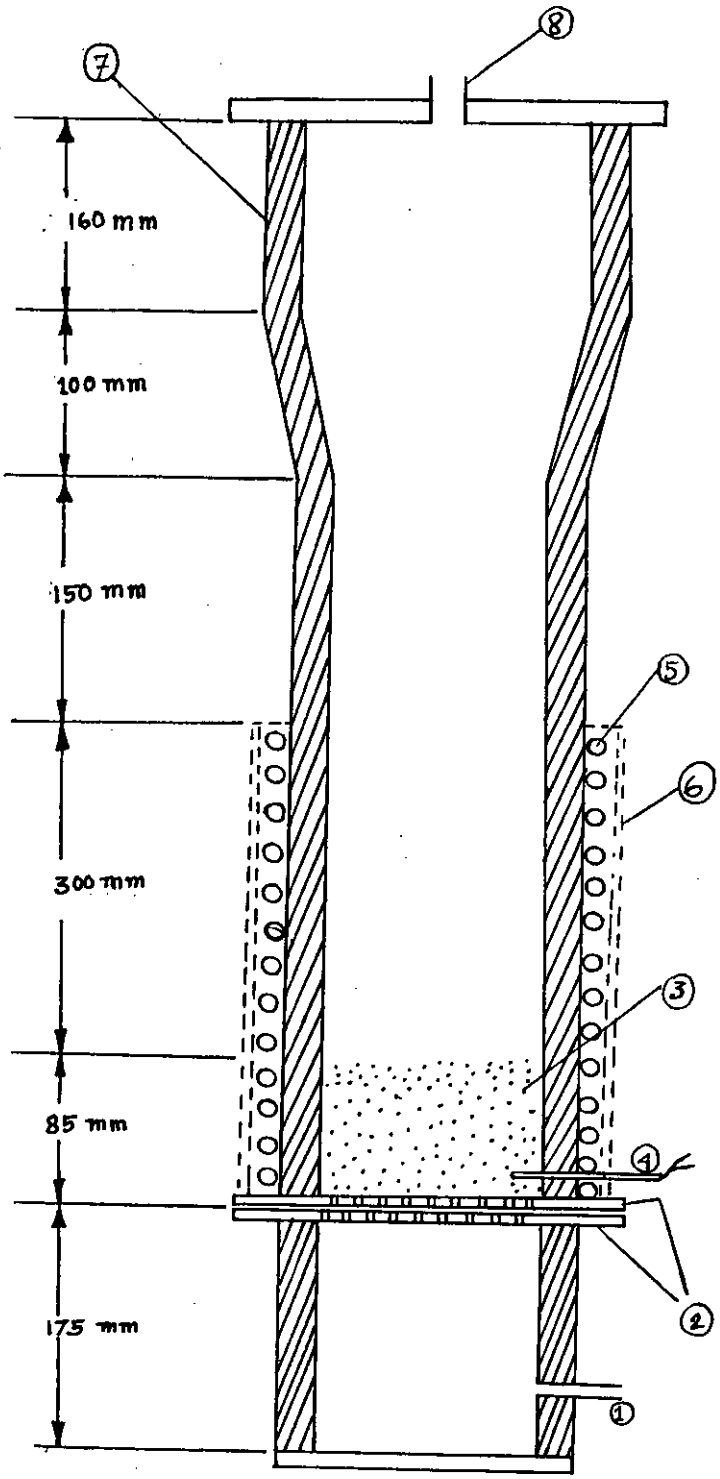

Fig. 3.2: Longitudinal Section View of the Reactor.

this exit line for sampling of products.

Hydrogen, nitrogen and carbon dioxide gases used in the study were obtained from Bangladesh Oxygen Limited. Streams from hydrogen, nitrogen and carbon dioxide lines were mixed in the mixing section before entry into the fluidizing zone. Product gases were analysed by a Shimadzu gas chromatograph. For the given catalyst size, particle Reynolds number was 4.6. The schematic diagram of the experimental setup is shown in Fig. 3.1. A photograph of the experimental setup is also attached.

3.1.2 Distributor plate

The distributor consisted of two circular plates of equal dimension. The plates were three inches in diameter, one-eighth inch in thickness and had a large number of holes drilled into them. The holes were 1 mm in diameter. The holes were drilled in such a way that when the two plates were put in place, the holes in the two plates were staggered without any overlapping. A thin aluminium foil was placed between the plates. This served as a gasket and also provided a gap for the passage of gas. This arrangement of the plates had to be adopted because the catalyst particles were in the size range 170-200 mesh whereas the smallest available drill bit was 1/8 inch. The drilled holes were therefore too large for the catalyst particles. The two plates with their dimensions are sketched in Fig. 3.3A and 3.3B.

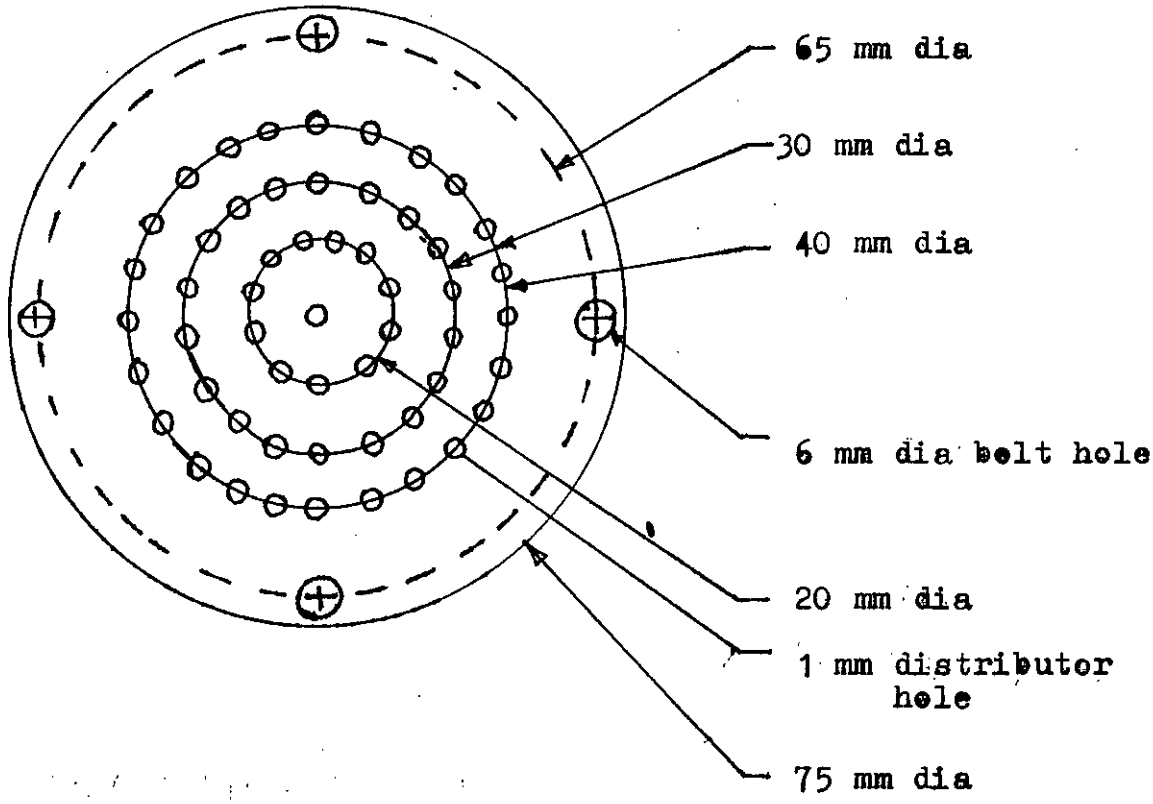

Fig. 3.3A: Upper Distributor Plate

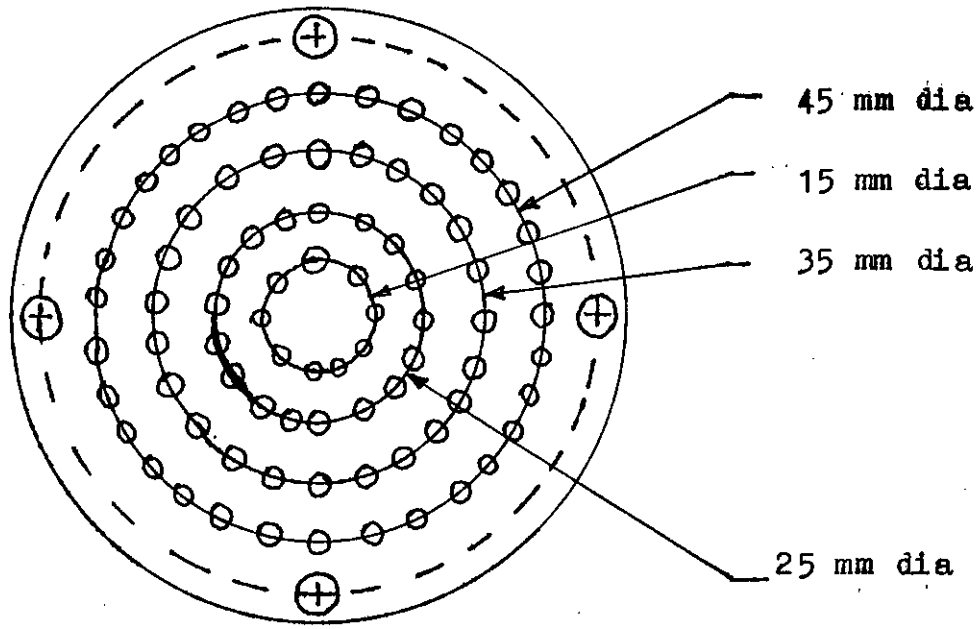

Fig. 3.3B: Lower Distributor Plate.

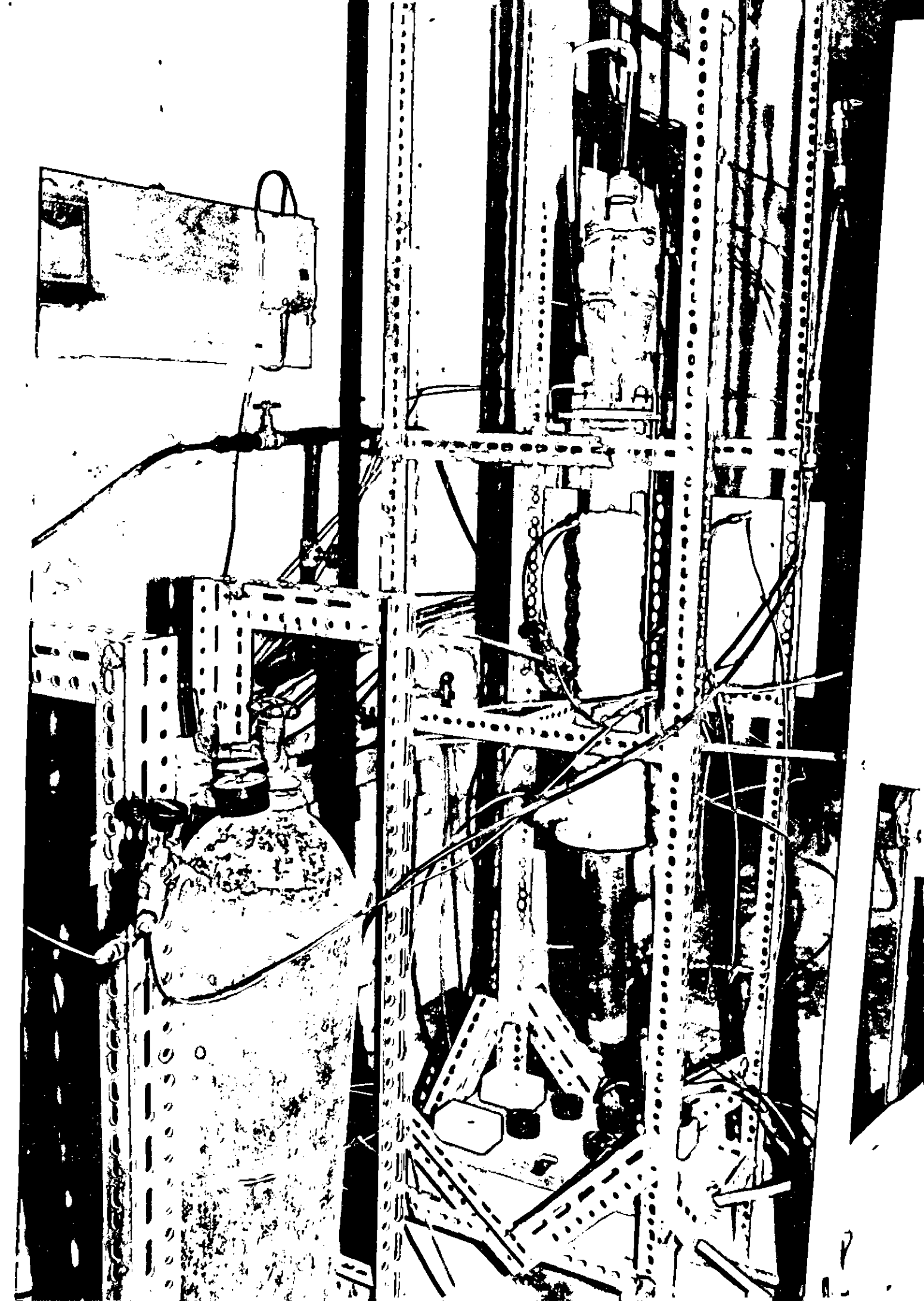

3.2 CATALYST

3.2.1 Preparation of catalyst

Alumina supported nickel catalyst is widely used for methanation reactions. In this work a 20% (w/w) of $Ni-Al_2O_3$ was prepared by the method of impregnation. 99.03 gm nickel nitrate ($Ni(NO_3)_2 . 6H_2O$) was taken in a beaker. Distilled water was added in an amount such that the resulting liquid volume was just enough to wet the support up to the point of incipient wetness. Alumina was then added into that nitrate solution with constant stirring of the slurry. When all the alumina was wetted the preparation was dried at 120°C for sixteen hours.

3.2.2 Calcination

The dried precursor of the catalyst was calcined in flowing nitrogen by the following steps:

(a) The catalyst and precursor were loaded into the reactor.

(b) Nitrogen was introduced at 100 ml/min.

(c) Temperature of the catalyst bed was raised to 120°C and kept there for two hours.

(d) The temperature was then raised to 400°C.

(e) At this temperature the catalyst was calcined for sixteen hours.

(f) The calcined catalyst was cooled to room temperature under nitrogen flow.

3.2.3 Reduction

The oxide form of the catalyst obtained by calcination is usually reduced to the active metal state by flowing hydrogen or hydrogen-nitrogen mixture at elevated temperatures. A considerable excess of hydrogen is required to sweep away the product water. In this study reduction was carried out in situ in the reactor and the following sequence was employed:

(a) A flow of 160 ml/min of a hydrogen : nitrogen mixture (ratio 3:1) was used. On a few occasions hydrogen was used instead of H_2-N_2 mixture.

(b) Temperature was raised to 120°C and held there for two hours.

(c) The temperature was then raised to 400°C and maintained for sixteen hours.

(d) The reduced catalyst was cooled under a reducing atmosphere i.e. either hydrogen flow or H_2-N_2 flow.

3.3 REACTION RUNS

On completion of reduction of the catalyst the reducing stream was replaced by the reactant stream of desired composition. The reactor bed was then fluidized by increasing the flow rate. When the desired flow rate was achieved the temperature was set to the desired level. Several chromatograms of the reaction products were then recorded. This procedure was repeated for all the reaction runs by varying the flowrate, composition or temperature.

CHAPTER FOUR

RESULTS & DISCUSSION

Methanation of carbon dioxide in fluidized bed reactor was carried out varying several parameters. Firstly, at constant temperature and with the same inlet composition, effect of variation of feed flow rate on the conversion of carbon dioxide was studied. Bed temperature was maintained at 240^{0}C and the inlet CO_2 composition was 6%. Prior to methanation runs the catalyst was reduced in hydrogen at 400^{0}C for 16 hours. Feed flow rate was varied from 424 ml/min to 1192 ml/min corresponding to superficial velocity of 1.4 cm/sec to 4.0 cm/sec. In the above range of inlet flowrate, it was found that the conversion of carbon dioxide is virtually unaffected. The plot of $\%CO_2$ conversion vs. inlet flowrate (Fig. 4.1) shows a conversion of 71.4% in the above flow range. The same experiment was conducted on a catalyst reduced with a mixture of hydrogen and nitrogen in the ratio of 3:1 and similar results were obtained as shown in Fig. 4.2.

This result gives the idea that change of inlet flow rate i.e. the average space velocity has no effect on the conversion of carbon dioxide. It is found from the study of Debruijin et. al (1) that with the increase of inlet flow rate i.e. space velocity conversion decreases gradually in a fixed bed reactor. In that case, at high space velocity the ratio of mass transport through the channel to mass transport by diffusion into the catalyst is relatively high, resulting in low carbon dioxide conversion. But in

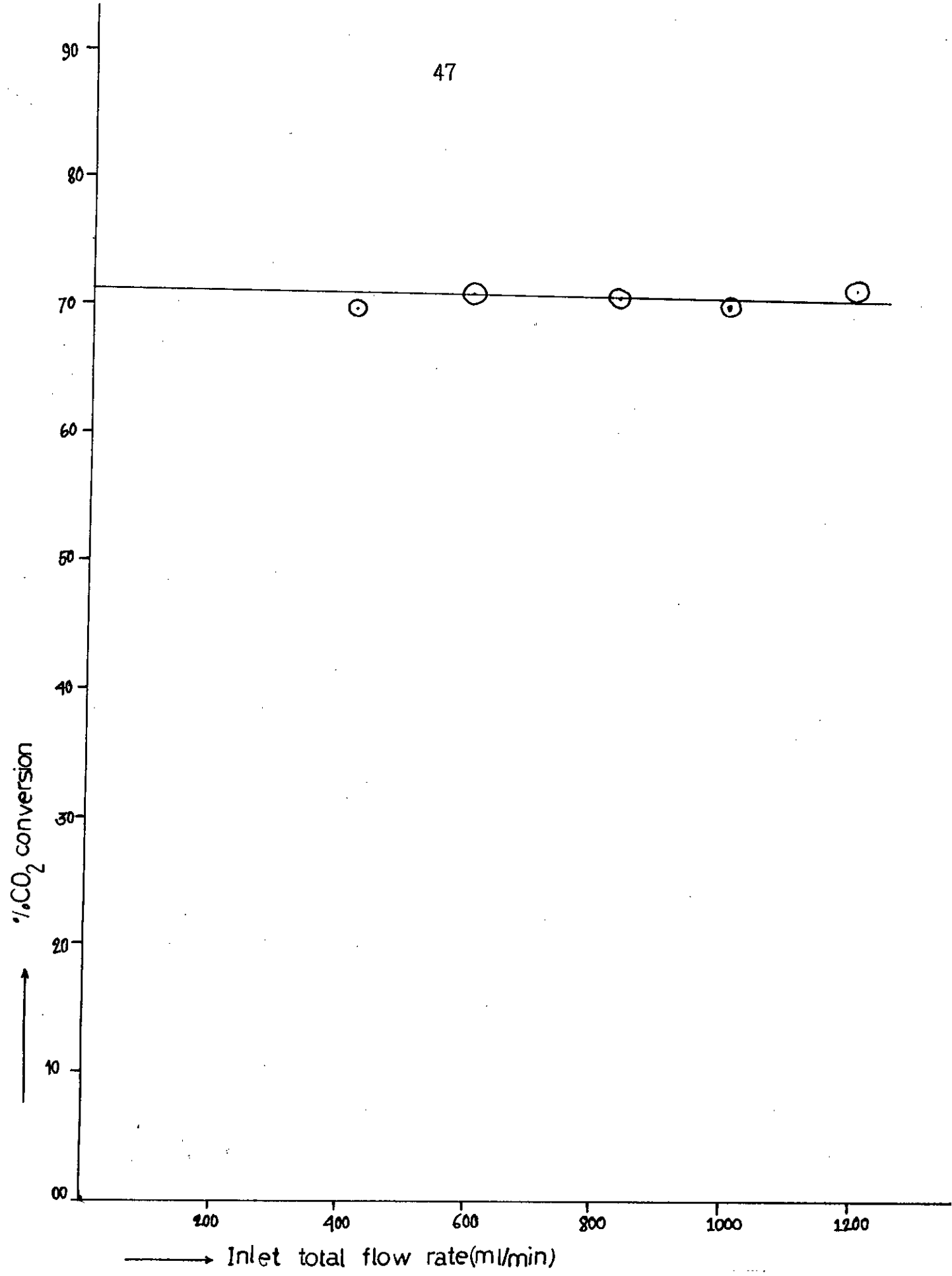

Fig. 4.1: Conversion of CO_2 vs. flow rate at const temperature and composition. Catalyst was reduced with hydrogen only.

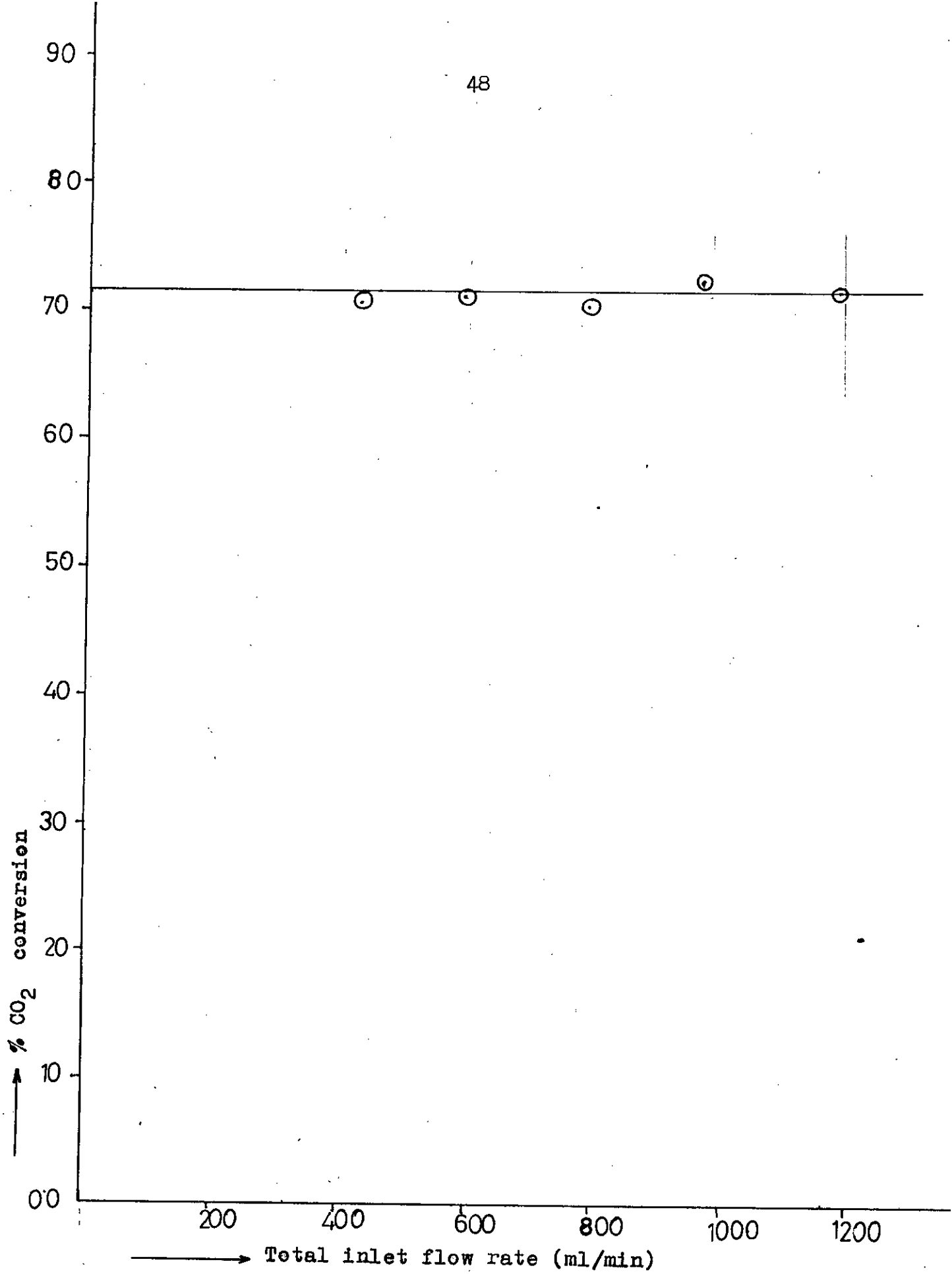

Fig. 4.2: Conversion of CO_2 vs. flow rate at const. temperature and composition. Catalyst was reduced with gas mixture of hydrogen to nitrogen ratio of 3:1.

fluidized beds, catalyst particles cover more volumes with larger height with the increase of flow rate. As a result, though residence time decreases gas molecules can get more time to coming contact with catalyst particles due to the increased volume of catalyst bed.

From the above result it is also found that reduction of catalyst with hydrogen at 400°C gives the same result. This is presumably because of the long duration of reduction, during which time the degree of reduction with pure hydrogen and 3:1 mixture of hydrogen and nitrogen may well be the same.

To study the effect of inlet carbon dioxide concentration on conversion, inlet carbon dioxide concentration was varied in the range of 2.6% to 7.8% at constant temperature and flow rate. Temperature was again maintained at 240°C. Carbon dioxide conversion was 77% at 2.6% inlet CO_2 concentration and this conversion decreased with increase of inlet CO_2 concentration. Carbon dioxide conversion decreased to 67.8% when inlet CO_2 concentration was 7.8%. This result is shown in Fig. 4.3.

From the study of Debuijn et. al. (1) it is found that at 224°C(497°K) bed temperature and 0.10 m^3/h space velocity conversion of CO_2 is 92%, 87% and 58% for inlet CO_2 concentration of 0.19%, 0.58% and 2.56% respectively. Van Herwijnen and et. al (6) used 2.38% inlet CO_2 concentration, 230°C bed temperature and obtained 60% CO_2 conversion for reciprocal space velocity of 50 (g.h/mol

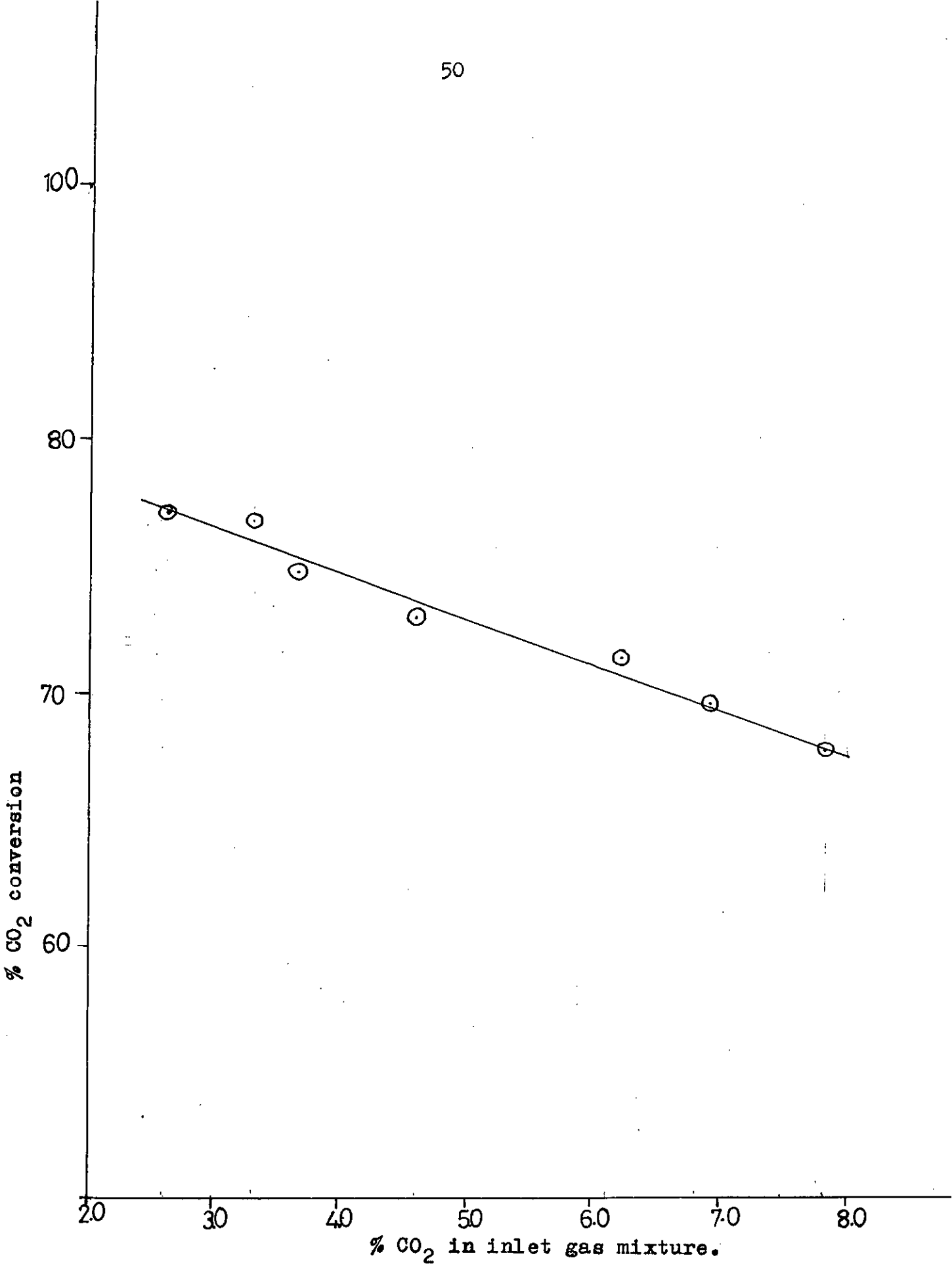

Fig. 4.3: Conversion of CO_2 vs. inlet composition of CO_2 at const temperature and flow rate.

CO_2). Dew et. al (14) used 20 to 30% carbon dioxide in the feed and they obtained carbondioxide conversion 10 to 20% only. All these previous work (1,6 & 14) described above clearly shows that conversion of carbondioxide decreases with the increase of CO_2 concentration in feed. In present work the conversions of 69.5 to 77% were achieved for a variation of inlet CO_2 concentration from 7.8 to 2.6% at a flow rate and temperature 450 ml/min and 240°C respectively. This is shown in fig. 4.3 and indicates that the observed behaviour is similar to those obtained in fixed-bed reactors under essentially similar operating conditions (1,6). This is due to the fact that with the increase of CO_2 in the feed, the ratio of H_2 to CO_2 decreases and consequently the conversion of CO_2 should be decreased. Similar results have been reported in fixed bed reactors (Fig. 2.10).

To study the effect of temperature another series of experiments was conducted by varying the temperature in the range of 210°C to 300°C at constant inlet composition and flow rate. Inlet CO_2 concentration was 2.6% and flow rate was 616 ml/min. Conversion of CO_2 was plotted against temperature as shown in fig. 4.4. It is found that with the increase of temperature, conversion gradually increased upto 240°C but after 240°C the rate of increase was lower. At 210°C, 240°C & 250°C conversion was 65.2%, 77% and 79.6% whereas at 300°C conversion was 80.6%. The experiment was repeated at an inlet CO_2 concentration of 3.6%, the flow rate being same as before. Similar results were obtained; at 210°C, 240°C & 250°C conversion was 64.6%, 74.7% and 76% respectively whereas at 300°C

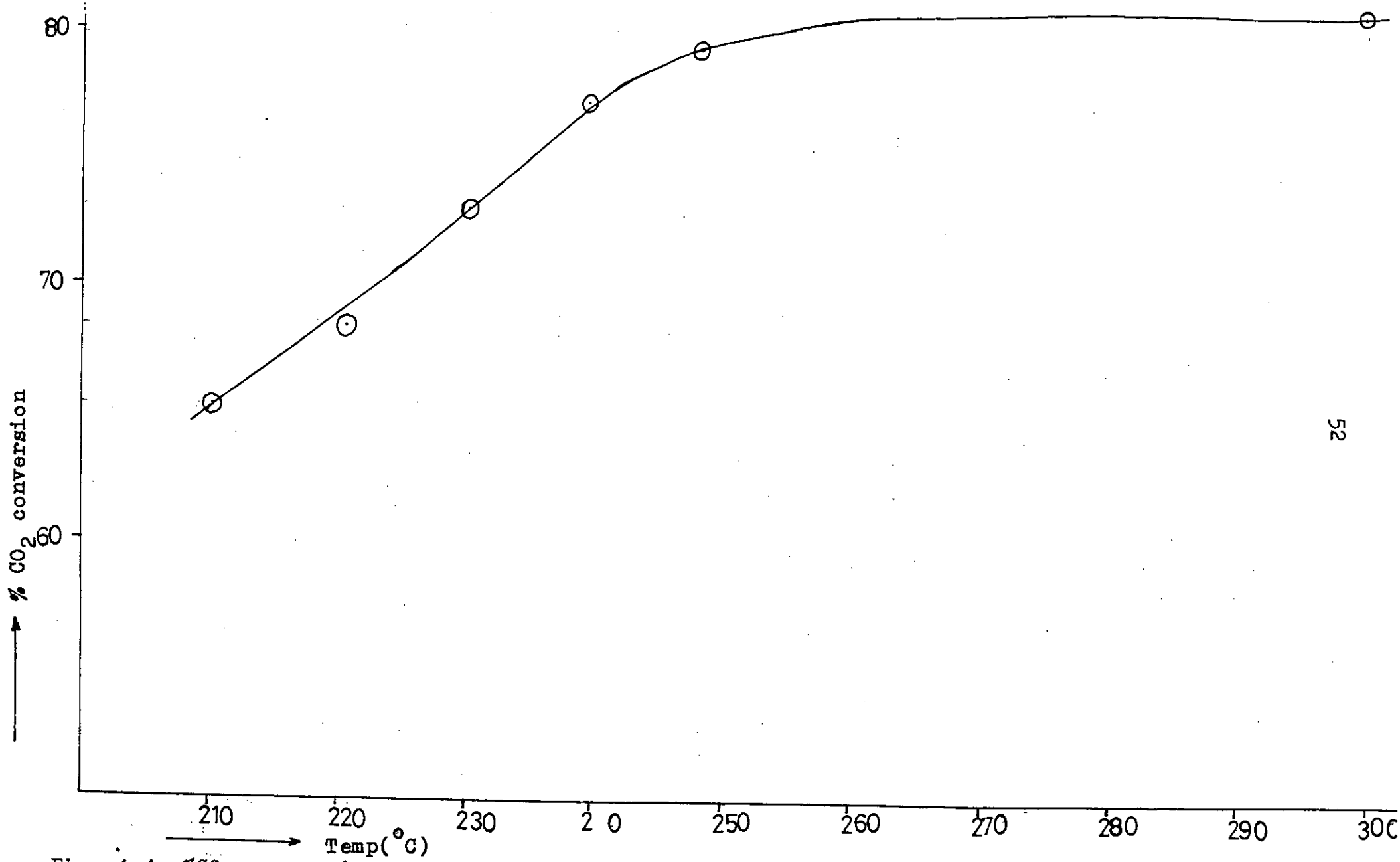

Fig. 4.4: %CO conversion vs. temperature at constant flowrate and const composition. Inlet CO_2 conc. 2.6%. Catalyst was reduced with hydrogen to nitrogen ratio 3:1

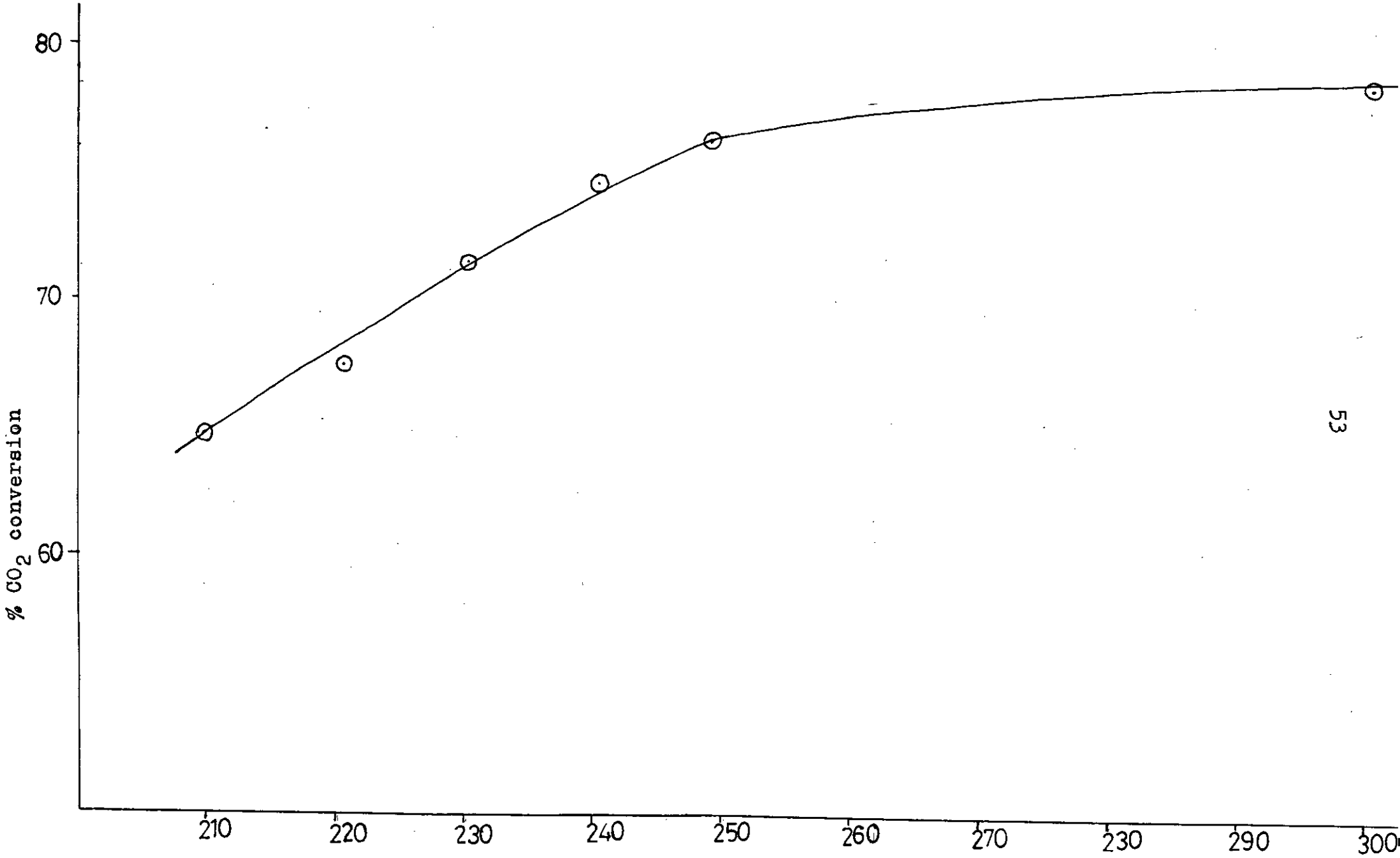

Fig. 4.5: % CO_2 conversion vs. temp. at const flow rate & composition. Inlet CO_2 conc 3.6% and catalyst was reduced with hydrogen to nitrogen ratio of 3:1.

conversion was 78.53%, which is shown in fig. 4.5.

From the results presented (fig. 4.4 and fig. 4.5) with temperature it is found that conversion of CO_2 increases monotonically up to a certain level then becomes constant. This isdue to the fact that although diffusion of the reactants into the catalyst pores and reaction rate both increases with temperature the increase of the latter is much more rapid than the former because of the fact the reaction rate increases exponentially with temperature whereas pore diffusion increase only as $(temperature)^{1/2}$. For this reason at the higher temperatures, diffusion resistance consumes more and more of the driving potential for transport of the reactants into the catalyst pores. As a result diffusion rate becomes controlling at the higher temperatures.

A series of experiments for methanation of CO_2 were carried out with unreduced catalyst. Calcined catalysts were used for the experiment, the reaction was started with 300^0c bed temperature, 2.6% inlet CO_2 concentration and hydrogen to nitrogen flow ratio 3:1. Chromatographic data regarding the experiment to determine outlet composition were collected at one hour intervals. Conversion of CO_2 was calculated for each run and was plotted against time of operation. This result is shown in fig. 4.6. It is found from this plot that conversion sharply rises to 42.2% within the first hour of operation, then it gradually increases up to 77% within the seventh hour of operation. After seven hours, the rate of increase becomes slower and becomes constant after about 11 hours. This

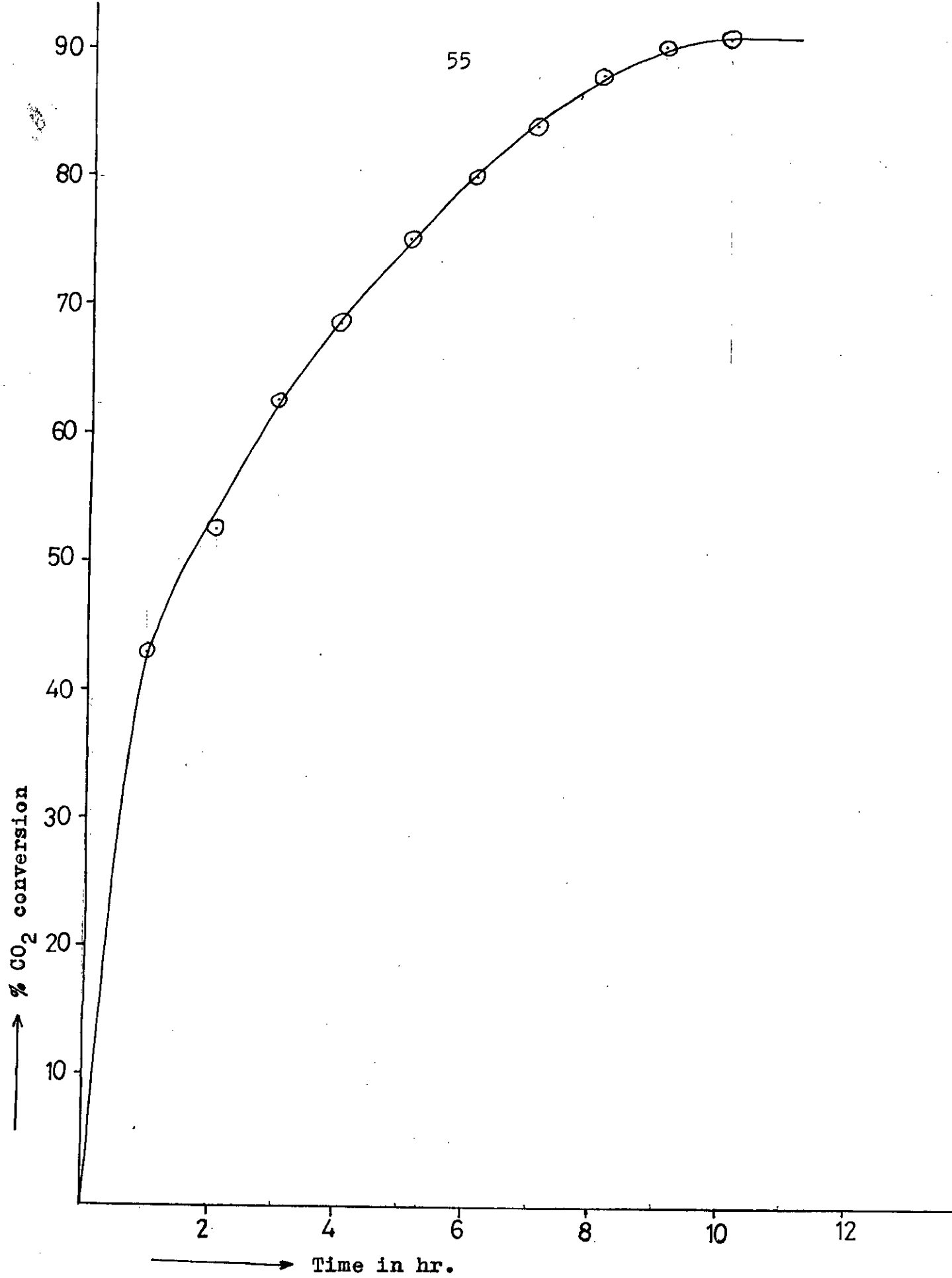

Fig. 4.6: Conversion of CO_2 vs. time at constant temperature, Composition. Catalyst was not prereduced.

result gives the idea that during the first seven hours reduction occurs very rapidly and as reduction proceeds, consequent higher conversions, are achieved. In this period i.e. in the first seven hours most of the NiO is reduced and the remainder, presumably a small fraction is reduced in the subsequent four hours, which explains the lower rate of increase of conversion during this period. After 11 hours conversion was 80.6% which is identical with the conversion obtained from the reaction carried out using same parameters and conditions but with a pre-reduced catalyst. One may conclude from this study that the time required for complete reduction of catalyst is much less than the 16 hrs used in this study. Furthermore, this time may well be even less than 11 hrs.

With a view to finding out activation energy (Ea) of the catalyst log of conversion against reciprocal temperature i.e. ln x vs. 1/T was plotted. According to the Arrhenius equation activation energy is obtained from a plot of ln k vs. 1/T. In this experiment a simplification has been made by reducing this plot to a plot of ln x vs. 1/T. This is possible by assuming zero order reaction. The most widely used kinetic equation for methanation is of the form $r = (kP_{CO_2})/(1+K_p P_{CO_2})$. In the temperature range of this study K_p is very large ($= 10^7$ atm^{-1}) so that for the concentration range of this study K_pP_{CO} is of the order of 10^5 i.e. $K_pP_{CO} >> 1$. Hence the above equation reduces to $r = k/K_p$ which is zero order. The plot of ln x vs. 1/T is derived as follows:

$$x = \frac{C_{in} - C_{out}}{C_{in}}$$

Or, $xC_{in} = C_{in} - C_{out}$
for a zero reaction
$C_{in} - C_{out} = kt$
$xC_{in} = kt$

$= A \exp(-Ea/RT)t$
Or, $\ln x + \ln C = \ln A - Ea/RT + \ln t$.

In this experiment the time was not a variable parameter. Hence a plot of lnx vs. 1/T would be a straight line with a slope = -Ea/R.

From this plot a straight line was obtained in the temperature range 210-250°C. From the slope (= -Ea/R), the activation energy was found to be 2.54 kcal/gmol. In the literature (9) reported activation energy for carbon dioxide methanation on nickel catalyst is 7 kcal/gmol for sufficiently low concentrations of CO_2 in the reactant stream. In the present study, however, the carbon dioxide concentration was 2.6-3.6% which is relatively high compared to industrial conditions. Since the rate constant is dependent on the concentration of CO_2, the activation energy will also depend on CO_2 concentration. At higher temperatures (250-300°C) deviation from linearity is observed in the plot of lnx vs. 1/T. This deviation may be attributed to the possible influence of mass transfer limitations at the high temperatures. For the very small particle size of catalysts used in this study it would appear that pore diffusion effects should be negligible. However using the same alumina support and a 20% Ni loading Ahmed (16) found that the pore size distribution of such a catalyst showed two peaks, one of which was in the small mesopore region. In such a case, pore diffusion resistance for the 50 μm size catalysts used in this study cannot be ruled out.

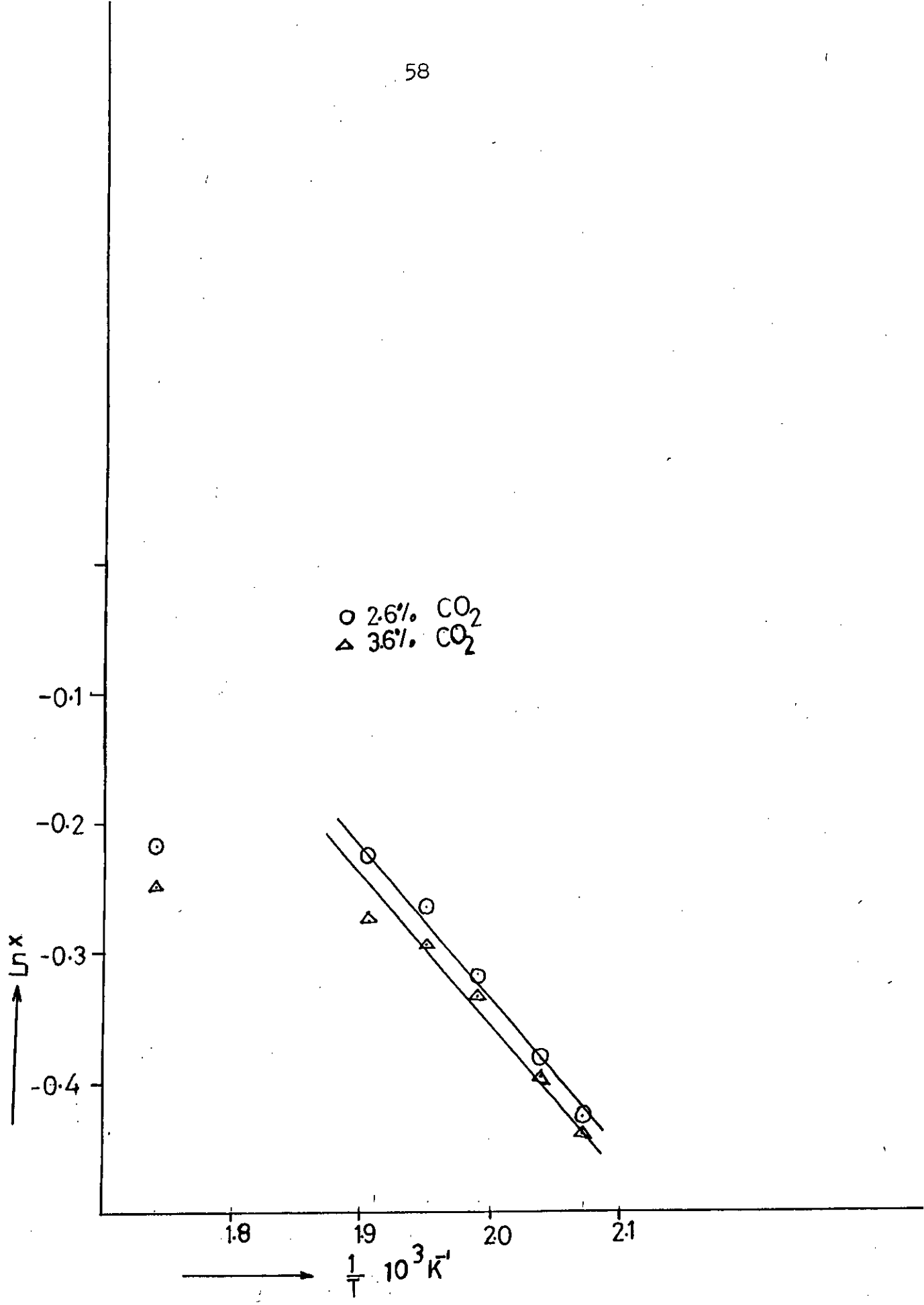

Fig. 4.7: Arrhenius Plot.

CHAPTER FIVE

CONCLUSION AND SUGGESTIONS

5.1 Conclusions

a) Conversion of carbon-dioxide does not vary in the flow range of 424 - 1192 ml/min for the reactor and bed height used in this work.

b) There is a significant effect of temperature on conversion of carbon dioxide. Starting from 210°C, conversion increases gradually up to 240°C, after which the increase rate is sluggish. Beyond 300°C the conversion is constant.

c) Conversion of carbon dioxide decreases with increase in carbon dioxide concentration in the reactant mixture at constant temperature.

d) Time required for complete reduction of catalyst is much less than the 16 hours used in this study. In fact, this time may well be less than 11 hours.

5.2 Suggestions for future work

This investigation was preliminary in nature whose aim was to study methanation of carbon dioxide in a fluidized bed. Methanation is an important industrial reaction which is at present being conducted in fixed beds. The methanation of carbon dioxide in fluidized bed can be considered as an alternative. This study has furnished some information but very limited to evaluate fully the performance of a fluidized methanator. The results of the present work points to

the need for continuing research endeavours in the following areas:

(a) The effect of catalyst size on methanation should be investigated.

(b) Catalyst weight should be changed to find out the effect of bed height on conversion.

(c) Good experimental data is needed to model fluidization for CO_2 methanation.

(d) With an aim to design fluidized bed reactors, parameters relevant to reactor design may be evaluated by combining experimental investigation with model building.

NOMENCLATURE

C	:	Concentration, gmols/cm^3.
C_p	:	Mols of product, gmols.
C_R	:	Mols of reactant, gmols.
$\overline{C}_p$	:	Heat capacity, cal/gmol.$^\circ$C.
C_1, C_2	:	Concentration in cloud and in void, gmols/cm^3.
D_p	:	Diameter of particle, micron.
Ea	:	Activation energy, kcal/gmol.
F	:	Feed rate, gm/sec.
g	:	Gravitational force, cm/sec^2.
$K_{p,CO2}$	:	Equilibrium constant for carbon dioxide, atm^{-2}.
k	:	Rate constant, cm^3/gcat.sec.
L	:	Bed height, mm.
U_b	:	Bubble velocity, cm/sec.
r	:	Reaction rate, gmols/gm.cat.sec.
U_o	:	Interstitial gas velocity, cm/sec.
U_t	:	Terminal settling velocity, cm/sec.
V_o	:	Superficial fluid velocity for fluidization, cm/sec.
V_{OM}	:	Minimum fluidization velocity, cm/sec.
V_1, V_2	:	Volumes of bubble cloud and void, cm^3.
W	:	Mass of catalyst in reactor, gms.
X_R	:	Conversion, gmols/gm of feed.
ρ	:	Density of fluid, gm/cm^3.

ρ_p : Density of particle, gm/cm^3.

μ : Viscosity, cp.

ϵ_N : Void fraction

α : Ratio of bubble velocity to intersticial gas velocity

ϕ_s : Spherical constant.

REFERENCES

1. V.K. Weekman, Jr. and Dan Luss. Chemical Reaction Engineering - Houston, ACS symposium series 65, 1978, p.63.

2. Hung M. Hulburt, Chemical Reaction Engineering-II, ACS symposium Series 133, 1974, p.489.

3. H. Van Doesburg and W.A. Dejong. Chemical Engg. Sc., 1976, Vol. 31, p.53.

4. H. Van Doesburg and W.A. Dejong. Chemical Engg. Sc., 1976, Vol. 31, p.45.

5. G.A. Mills and F.W. Steffgen, Chem. Res. Dev. 1974, Vol. 8, p.159.

6. T. Van Herwijnen and et. al., J. Cat 1973, Vol. 28, p.391.

7. Catalyst Seminar Paper June, 1978, Catalysts and Chemicals Inc; Far East Sankaido Btdg. 9-13, Akasaka 1-Chome, Minato-Ku, Tokyo, Japan.

8. Review work done by G. Alex Mills and Fred W. Steffgen and reported in Chemical Rev (1974), Vol. 8, U.S. Bureau of Mines Washington, D.C. 20240.

9. ICI Catalyst Handbook, Wolfe Scientific Publication Co. Ltd., UK, 1970, p.115.

10. "Short Course on Industrial Catalysts and Chemical Reactors" - Jan 22-28, BUET, 1984

11. R.F. Gould, Chemical Reaction Engg. ACS symposium Series 109, 1972, p.106.

12. W.L. McCabe and J.C. Smith. Unit Operations of Chemical Engg., 3rd 3d. p.159.

13. J.F. Davidson, R. Cliff and D. Harrison, "Fluidization" 2nd ed. Academic Press, London, 1985 P.595.

14. J.N. Dew, R.R. White, and C.M. Sliepcevich. Industrial and Engg. Chem., 1978, Vol. 47, No. 1. P.140-146.

15. Jeng H. Chlang and Jack R. Hoppwer. Ind. Eng. Chem. Prod. Res. Dev. 1983, Vol. 22, p.225.

16. K. Ahmed, "Influence of Preparation Variables on the Proporties of the Methanation Catalyst", Final Report, CASR Project No. 68/111/88, BUET, 1989.

APPENDIX

Table 7.1A: Collected data varying flow rate at const. temp. and composition.

Run No.	Temp. (°C)	Compo-nent	Flow rate (ml/min)	% volume	Total flow rate (ml/min)
1	240	CO_2	24	5.7	424
		H_2	300	70.7	
		N_2	100	23.6	
2	240	CO_2	36	6.0	596
		H_2	420	70.5	
		N_2	140	23.5	
3	240	CO_2	48	6.0	808
		H_2	570	70.5	
		N_2	190	23.5	
4	240	CO_2	60	6.1	980
		H_2	690	70.4	
		N_2	230	23.5	
5	240	CO_2	72	6.0	1192
		H_2	840	70.5	
		N_2	280	23.5	

Table 7.1B: Collected data varying flow rate at const. temp. and composition. Catalyst was reduced with hydrogen only.

Run No.	Peak position	COLUMN-2 H_2	N_2	CH_4	CO	COLUMN-1 (H_2+N_2+CH_4+CO)	CO_2
	Atn[1]	32	256	32	2.0	512	8.0
1	Ph[2]	63	40.2	52.8	37.5	32.5	49.3
	Pw[3]	2.0	6.8	6.0	5.5	11.0	13.0
	Atn	32	256	32	2.0	512	8.0
2	Ph	84.4	51.5	71.3	49.8	43.5	63.3
	Pw	2.0	7.0	6.5	5.5	11.0	13.5
	Atn	64	256	32	2.0	512	16.0
3	Ph	57.9	64	89.7	60	58	43.9
	Pw	2.0	7.5	7.0	6.0	11.0	12.5
	Atn.	64	256	64	2.0	512	16.0
4	Ph	79.7	80	70.8	68.5	69.5	56.4
	Pw	2.0	8.0	6.0	6.2	11.8	13.0
	Atn.	64	256	64.0	2.0	512	32.0
5	Ph	94.2	97	84.4	73.5	92	38.9
	Pw	2.2	8.8	6.7	6.5	12.0	12.0

1 Attennation.
2 Peak height.
3 Peak height at half height.

Table 7.1C: Calculated data of the collected data varying flow rate at const. temp. & composition.

Run No.	Coln.	Component	K_F	Area	% Volume (dry basis)	% Volume in outlet (dry basis)	Component flowrate (ml/min)	$\%CO_2$ conversion
1	2	H_2	36	145152	64.30	62.89	207.4	
		N_2	1.0	69980.16	31.00	30.32	100.0	
		CH_4	1.0	10137.6	4.49	4.39	14.48	
		CO	1.1	3466.125	0.21	0.21	0.69	
	1	$(H_2+N_2+CH_4+CO)$	1.0	183040	97.81			
		CO_2	0.8	4107.76	2.19	2.19	7.2	70
2	2	H_2	36	194457.6	64.35	62.95	295.0	
		N_2	1.0	92288	30.54	29.87	140.0	
		CH_4	1.0	14830.4	4.91	4.80	22.5	
		CO	1.13	619.0	0.20	0.20	0.94	
	1	$(H_2+N_2+CH_4+CO)$	1.0	244992	97.82			
		CO_2	0.8	5469.12	2.18	2.18	10.22	71.6
3	2	H_2	36	266803.2	65.00	63.64	412.7	
		N_2	1.0	122880	29.93	29.30	190.0	
		CH_4	1.0	20092.8	4.89	4.79	31.1	
		CO	1.13	720.0	0.18	0.18	1.17	
	1	$(H_2+N_2+CH_4+CO)$	1.0	315392	97.9			
		CO_2	0.8	7024	2.1	2.10	13.62	71.6

Run No.	Coln.	Component	K_F	Area	% Volume (dry basis)	% Volume in outlet (dry basis)	Component flowrate (ml/min)	$\%CO_2$ conversion
4	2	H_2	36	367257.6	65.67	64.23	512.45	
		N_2	1.0	163840	29.30	28.66	230.0	
		CH_4	1.0	27187.2	4.86	4.75	38.12	
		CO	1.13	959.82	0.17	0.17	1.38	
	1	$(H_2+N_2+CH_4+CO)$	1.0	419891.2	97.81			
		CO_2	0.8	9384.96	2.19	2.19	17.58	70.7
5	2	H_2	36	477480.96	65.12	63.77	611.9	
		N_2	1.0	218521.6	29.80	29.18	280.04	
		CH_4	1.0	36190.72	4.94	4.84	46.44	
		CO	1.13	1079.715	0.15	0.15	1.44	
	1	$(H_2+N_2+CH_4+CO)$	1.0	565248	97.93			
		CO_2	0.8	11950.0	2.07	2.07	19.86	72.4

TABLE 7.2A: COLLECTED DATA VARING FLOW RATE AT CONST. TEMP AND COMPOSITION.

Run No.	Temp. (°C)	Component	Flow rate (ml/min)	% Volume	Total flow rate (ml/min)
1	240	CO_2	24	5.7	424
		H_2	300	70.7	
		N_2	100	23.6	
2	240	CO_2	36	6.0	596
		H_2	420	70.5	
		N_2	140	23.5	
3	240	CO_2	48	6.0	808
		H_2	570	70.5	
		N_2	190	23.5	
4	240	CO_2	60	6.1	980
		H_2	690	70.4	
		N_2	230	23.5	
5	240	CO_2	72	6.0	1192
		H_2	840	70.5	
		N_2	280	23.5	

Table 7.2B: Collected data varying flow rate at const. temperature and composition. Catalyst was reduced with the gas mixture of hydrogen to nitrogen ratio of 3:1.

Run No.	Peak position	COLUMN - 2				COLUMN - 1	
		H_2	N_2	CH_4	CO	$(H_2+N_2+CH_4+CO)$	CO_2
	Atn.	32	256	32	2.0	512	8.0
1	Ph	62.7	42.0	51.1	38	32	48
	Pw	2.0	6.5	6.2	5.5	11.0	12.5
	Atn.	32	256	32	2.0	512	8.0
2	Ph	83	52	70.8	48.5	43	64.8
	Pw	2.0	7.0	6.6	5.5	11.0	13.4
	Atn.	32	256	32	2.0	512	16
3	Ph	91.4	65	90.9	53.6	55	47.9
	Pw	2.5	7.5	7.0	6.0	11.5	12.0
	Atn.	64	256	64	2.0	512	16
4	Ph	76.6	80.1	66.2	63.5	70.5	54.1
	Pw	2.0	7.8	6.5	6.4	12	13.4
	Atn.	64	256	64	4.0	512	32
5	Ph	89.5	95.0	81.0	49.3	87.84	39.4
	Pw	2.3	8.8	7.0	5.5	12.5	12.0

TABLE 7.2C: CALCULATED DATA FROM COLLECTED DATA AT CONST. TEMP. AND COMPOSITION.

Run No.	Coln.	Component	K_p	Area	% Volume (dry basis)	% Volume in outlet (dry basis)	Component flowrate (ml/min)	$\%CO_2$ conversion
1	2	H_2	36	14460.8	64.2	62.88	206.7	
		N_2	1.0	69888	31.07	30.42	100.0	
		CH_4	1.0	10138.24	4.51	4.41	14.5	
		CO	1.13	472.34	0.21	0.21	0.7	
	1	$(H_2+N_2+CH_4+CO)$	1.0	180224	97.91			
		CO_2	0.8	3840	2.09	2.09	6.87	71.4
2	2	H_2	36	191232	63.81	62.38	287.3	
		N_2	1.0	93184	31.10	30.40	140.0	
		CH_4	1.0	14952.96	4.99	4.88	22.5	
		CO	1.13	301.43	0.10	0.10	0.5	
	1	$(H_2+N_2+CH_4+CO)$	1.0	242176	97.76			
		CO_2	0.8	5557.25	2.24	2.24	10.31	71.36
3	2	H_2	36	263232	64.74	62.91	400.8	
		N_2	1.0	124800	30.50	29.82	190.0	
		CH_4	1.0	20361.6	4.98	4.87	31.03	
		CO	1.13	726.82	0.18	0.18	1.2	
	1	$(H_2+N_2+CH_4+CO)$	1.0	323840	97.78			
		CO_2	0.8	7357.44	2.22	2.22	14.14	70.54

Run No.	Coln:	Component	K_p	Area	% Volume (dry basis)	% Volume in outlet (dry basis)	Component flowrate (ml/min)	$\%CO_2$ conversion
4	2	H_2	36	352972.8	65.20	63.83	507.6	
		N_2	1.0	159943.6	29.54	28.92	230.0	
		CH_4	1.0	27539.2	5.09	4.98	39.6	
		CO	1.13	918.50	0.17	0.17	1.35	
	1	$(H_2+N_2+CH_4+CO)$	1.0	433152	97.90			
		CO_2	0.8	9296.38	2.10	2.10	16.7	72.2
5	2	H_2	36	474278.4	65.34	63.96	620.1	
		N_2	1.0	214016.0	29.49	28.88	280.0	
		CH_4	1.0	36288.0	5.0	4.89	47.41	
		CO	1.13	1225.6	0.17	0.17	1.65	
	1	$(H_2+N_2+CH_4+CO)$	1.0	562176	97.89			
		CO_2	0.8	12103.68	2.11	2.11	20.46	71.62

TABLE 7.3A: COLLECTED DATA VARYING COMPOSITION AT CONST. TEMP.

Run No.	Temp. (^{0}C)	Flow rate H_2(ml/min)	Flow rate of N_2(ml/min)	Flow rate of CO_2(ml/min)	% Volume of CO_2
1	240	450	150	16	2.6
2	240	450	150	20	3.2
3	240	450	150	22.5	3.6
4	240	450	150	29	4.6
5	240	450	150	39	6.1
6	240	450	150	44	6.8
7	240	450	150	51	7.8

TABLE 7-3B: COLLECTED DATA VARYING COMPOSITION AT CONSTANT TEMP. AND FLOW RATE.

Run No.	Peak Position	COLUMN - 2				COLUMN - 1	
		H_2	N_2	CH_4	CO	$(H_2+N_2+CH_4+CO)$	CO_2
	Atn.	32	256	16.0	2.0	512	4
1	Ph	80.2	50.0	71.0	36.5	40.2	49.6
	Pw	2.0	6.9	5.5	5.5	11.0	13.0
	Atn.	32	256	16	2.0	512	4
2	Ph	79.2	51.0	86.8	35.5	40.0	53.7
	Pw	2.0	6.9	6.0	5.5	11.0	13.0
	Atn.	32	256	16	2.0	512.0	4.0
3	Ph	74.2	49.4	92.8	38.0	41.0	65.80
	Pw	2.0	6.9	6.0	5.5	11.0	13.5
	Atn.	32	256	32	2.0	512.0	8
4	Ph	74.2	49	53.2	38.2	42.5	48.7
	Pw	2.0	6.9	7.0	5.5	11.0	12.7
	Atn.	32	256	32	2.0	512	8
5	Ph	68.6	49.0	69.6	41.0	43.0	68.8
	Pw	2.0	6.9	7.0	5.5	11.0	13.5
	Atn.	32	256	32.0	2.0	512	8
6	Ph	66.6	48.6	76.4	42.0	43.5	78.3
	Pw	2.0	6.9	7.0	6.0	11.0	13.0

TABLE 7-3C: Calculated data from collected data varying composition at constant temperature.

Run No.	Column	Component	K_p	Area	%Volume in each colm.(dry basis)	%Volume in outlet (dry basis)	Component flowrate (ml/min)	$\%CO_2$ conversion
1	2	H_2	36	194227.2	65.92	65.41	312.67	
		N_2	1.0	93184.0	31.62	31.38	150.00	
		CH_4	1.0	6820.0	2.31	2.29	10.95	
		CO	1.13	422.62	0.14	0.14	0.69	
	1	$(H_2+N_2+CH_4+CO)$	1.0	222464	99.23			
		CO_2	0.8	1732.0	0.77	0.77	3.68	77
2	2	H_2	36	182476.8	64.86	64.22	303.78	
		N_2	1.0	90080.4	32.02	31.71	150.00	
		CH_4	1.0	8332.8	2.96	2.93	13.86	
		CO	1.13	441.265	0.16	0.16	0.76	
	1	$(H_2+N_2+CH_4+CO)$	1.0	225280	99.02			
		CO_2	0.8	2233.92	0.98	0.98	4.64	76.8
3	2	H_2	36	172108.8	64.04	63.26	295.88	
		N_2	1.0	87260.16	32.47	32.07	150.00	
		CH_4	1.0	8908.8	3.31	3.27	15.29	
		CO	1.13	472.345	0.18	0.18	0.84	
	1	$(H_2+N_2+CH_4+CO)$	1.0	230912	98.78			
		CO_2	0.8	2844.72	1.22	1.22	5.7	74.7

Run No.	Column	Component	K_p	Area	%Volume in each colm.(dry basis)	%Volume in outlet (dry basis)	Compo-nent flow (ml/min)	$\%CO_2$ conver-sion
4	2	H_2	36	170956.8	63.35	62.31	296.53	
		N_2	1.0	86553.6	32.05	31.53	150.00	
		CH_4	1.0	11916.8	4.42	4.35	20.70	
		CO	1.13	472.34	0.17	0.17	0.8	
	1	$(H_2+N_2+CH_4+CO)$	1.0	237670.4	98.36			
		CO_2	0.8	3958.33	1.64	1.64	7.8	73.1
5	2	H_2	36	158054.4	60.63	59.17	274.03	
		N_2	1.0	86553.6	33.20	32.40	150.00	
		CH_4	1.0	15590.4	5.98	5.84	27.04	
		CO	1.13	509.64	0.19	0.19	0.88	
	1	$(H_2+N_2+CH_4+CO)$	1.0	242176.4	97.60			
		CO_2	0.8	5948.83	2.40	2.40	11.11	71.5
6	2	H_2	36	153446.4	59.73	58.07	268.3	
		N_2	1.0	85847.04	33.40	32.43	150.00	
		CH_4	1.0	17113.6	6.65	6.46	29.88	
		CO	1.13	569.52	0.22	0.21	0.97	
	1	$(H_2+N_2+CH_4+CO)$	1.0	244992	97.10			
		CO_2	0.8	7316.33	2.90	2.90	13.41	69.52
7	2	H_2	36	15275524	59.43	57.33	267.6	
		N_2	1.0	85670.4	33.32	32.14	150.00	
		CH_4	1.0	18076.8	7.03	6.78	31.64	
		CO	1.13	573.58	0.22	0.21	0.98	
	1	$(H_2+N_2+CH_4+CO)$	1.0	29446.4	96.46			
		CO_2	0.8	9152	3.54	3.54	16.52	67.62

Table 7.4.A: Collected data varying temperature at constant composition and flowrate.

Run No.	Component	Flowrate(ml/min)	%volume
1 to 6	CO_2	16	2.6
	H_2	450	73.1
	N_2	150	24.3

Table 7.4B: Collected data varying temperature at const. composition and flow rate.

Run No.	Temp. (°C)	Peak Position	COLUMN - 2 H_2	N_2	CH_4	CO	COLUMN - 1 (H_2+N_2+CH_4+CO)	CO_2
		Atn.	32	256	16	2.0	512	4.0
1	210	Ph	75	47	56.3	39	41.5	61.6
		Pw	2.0	6.5	5.0	5.6	11.0	13.5
		Atn.	32	256	16	2.0	512	4.0
2	220	Ph	79.7	49	65.1	38	40.8	57.0
		Pw	2.0	6.9	5.0	5.5	11.0	13.4
		Atn.	32	256	16	2.0	512	4.0
3	230	Ph	80.2	50	71.0	36.5	40.2	49.6
		Pw	2.0	6.9	5.5	5.5	11.0	13.0
		Atn.	32	256	16	2.0	512.0	4.0
4	240	Ph	84.3	52	77.5	34	39.5	43.3
		Pw	2.0	7.0	5.5	5.5	11.0	12.5
		Atn.	32	256	16	1.0	512	4.0
5	250	Ph	87.5	54.7	81	44	39.0	40.0
		Pw	2.0	7.0	6.0	6.0	11.0	12.0
		Atn.	32	256	16	1.0	512	4.0
6	300	Ph	88.4	57.5	89.8	41	37.0	36.6
		Pw	2.0	7.0	6.0	6.0	11.0	12.0

Table 7.4C: Calculated data from collected data varying temperature at constant composition.

Run No.	Column	Component	k_f	Area	%volume in each column (dry basis)	%volume in outlet (dry basis)	Component flow rate in outlet (ml/min)	$\%CO_2$ conversion
1	2	H2	36	172800	67.50	66.74	331.38	
		N_2	1.0	78208	30.55	30.21	150.0	
		CH_4	1.0	4500	1.76	1.74	8.64	
		CO	1.13	493.584	0.19	0.19	0.94	
	1	$(H_2+N_2+CH_4+CO)$	1.0	233728	98.88			
		CO_2	0.8	2661.12	1.12	1.12	5.56	65.25
2	2	H_2	36	183628	66.56	65.85	318.28	
		N_2	1.0	86553.6	31.38	31.05	150.0	
		CH_4	1.0	5208	1.89	1.87	9.03	
		CO	1.13	472.38	0.17	0.17	0.82	
	1	$(H_2+N_2+CH_4+CO)$	1.0	229785.6	98.95			
		CO_2	0.8	2444.16	1.05	1.05	5.07	68.3
3	2	H_2	36	184780.8	66.04	65.45	313.76	
		N_2	1.0	88320	31.57	31.29	150.0	
		CH_4	1.0	6248	2.23	2.21	10.6	
		CO	1.13	453.69	0.16	0.16	0.77	
	1	$(H_2+N_2+CH_4+CO)$	1.0	226406.4	99.10			
		CO_2	0.8	2063.36	0.90	0.90	4.31	73.0

Run No.	Column	Component	k_p	Area	%volume in each column (dry basis)	%volume in outlet (dry basis)	Component flow rate in outlet (ml/min)	$\%CO_2$ conversion
4	2	H_2	36	194227.2	65.92	65.41	312.67	
		N_2	1.0	93184	31.62	31.38	150.0	
		CH_4	1.0	6820	2.31	2.29	10.95	
		CO	1.13	422.62	0.14	0.14	0.67	
	1	$(H_2+N_2+CH_4+CO)$	1.0	222464.4	99.23			
		CO_2	0.8	1732	0.77	0.77	3.68	77
5	2	H_2	36	201600	65.51	66.067	308.4	
		N_2	1.0	98022.4	31.86	31.64	150.0	
		CH_4	1.0	7776	2.53	2.51	11.90	
		CO	1.13	298.32	0.10	0.10	0.47	
	1	$(H_2+N_2+CH_4+CO)$	1.0	219648	99.31			
		CO_2	0.8	1536	0.69	0.69	3.27	79.6
6	2	H_2	36	203558.4	64.52	64.09	296.35	
		N_2	1.0	9103040	32.66	32.44	150.0	
		CH_4	1.0	8620.8	2.73	2.71	12.53	
		CO	1.13	277.98	0.09	0.09	0.42	
	1	$(H_2+N_2+CH_4+CO)$	1.0	208384	99.33			
		CO_2	0.8	1405.44	0.67	0.67	3.1	80.6

Table 7.5A: Collected data varying temp. at const. composition and flow rate.

Run No.	Component	Flowrate(ml/min)	%volume
1 to 6	CO_2	22.5	3.6
	H_2	450.0	72.3
	N_2	150.0	24.1

Table 5B: Collected data varying temperature at const composition and flow rate.

Run No.	Temp. (^{0}C)	Peak Position	COLUMN - 2 H_2	N_2	CH_4	CO	COLUMN - 1 (H_2+N_2+CH_4+CO)	CO_2
1	210	Atn.	32	256	16.0	2.0	512	4.0
		Ph	73	46.5	74.2	41.5	42.5	78.1
		Pw	2.0	6.8	5.5	5.6	11.0	15.0
2	220	Atn.	32	256	16	2.0	512	4.0
		Ph	74	47	78.7	40.5	42.5	77.9
		Pw	2.0	6.9	5.7	5.6	11.0	13.4
3	230	Atn.	32	256	16	2.0	512	4.0
		Ph	75.2	48.5	80.9	39	41.8	73.2
		Pw	2.0	6.9	6.0	5.6	11.0	14.0
4	240	Atn.	32	256	16	2.0	512.0	4.0
		Ph	74.7	49.4	92.8	38	41.0	65.85
		Pw	2.0	6.9	6.0	5.5	11.0	13.5
5	250	Atn.	32	256	16	2.0	512	4.0
		Ph	76.7	50.5	93	36.4	41.0	62.0
		Pw	2.0	6.9	6.0	5.5	11.0	13.5
6	300	Atn.	32	256	16	2.0	512	4.0
		Ph	78.4	52.2	97.5	34	39.4	56
		Pw	2.0	6.9	6.0	5.5	11.0	13.0

Table 7.5C: Calculated data from collected data varying temperature at constant composition.

Run No.	Column	Component	k_p	Area	%volume in each column (dry basis)	%volume in outlet (dry basis)	Component flow rate in outlet (ml/min)	$\%CO_2$ conv.
1	2	H_2	36	168192	65.65	64.57	311.63	
		N_2	1.0	80947.2	31.60	31.08	150.0	
		CH_4	1.0	65.29.6	2.55	2.51	12.11	
		CO	1.13	525.22	0.20	0.20	0.96	
	1	$(H_2+N_2+CH_4+CO)$	1.0	239360	98.35			
		CO_2	0.8	4022.56	1.65	1.65	7.96	64.6
2	2	H_2	36	170496	65.27	64.26	308.18	
		N_2	1.0	83020.8	31.78	31.29	150.0	
		CH_4	1.0	7177.44	2.75	2.71	12.99	
		CO	1.13	512.57	0.20	0.20	0.96	
	1	$(H_2+N_2+CH_4+CO)$	1.0	239360	98.46			
		CO_2	0.8	3748.8	1.54	1.54	7.38	67.2
3	2	H_2	36	172800	64.78	63.89	302.5	
		N_2	1.0	85670.4	32.12	31.68	150.0	
		CH_4	1.0	7766.4	2.91	2.87	13.59	
		CO	1.13	493.58	0.19	0.19	0.90	
	1	$(H_2+N_2+CH_4+CO)$	1.0	235417.6	98.63			
		CO_2	0.8	3279.36	1.37	1.37	6.49	71.15

Run No.	Column	Component	k_p	Area	%volume in each column (dry basis)	%volume in outlet (dry basis)	Component flow rate in outlet (ml/min)	$\%CO_2$ conv.
4	2	H_2	36	172108.8	64.04	63.26	295.88	
		N_2	1.0	987260.16	32.47	32.07	150.0	
		CH_4	1.0	8908.8	3.31	3.27	15.29	
		CO	1.13	472.34	0.18	0.18	0.84	
	1	$(H_2+N_2+CH_4+CO)$	1.0	230912	98.78			
		CO_2	0.8	2844.72	1.22	1.22	5.7	74.7
5	2	H_2	36	176716.8	64.20	63.46	297.28	
		N_2	1.0	89203.2	32.39	32.02	150.0	
		CH_4	1.0	8928	3.24	3.20	14.99	
		CO	1.13	452.45	0.16	0.16	0.75	
	1	$(H_2+N_2+CH_4+CO)$	1.0	230912	98.85			
		CO_2	0.8	2678.4	1.15	1.15	5.39	76
6	2	H_2	36	180633.6	63.91	63.25	293.82	
		N_2	1.0	92206	32.63	32.29	150.0	
		CH_4	1.0	9360	3.31	3.28	15.24	
		CO	1.13	422.62	0.15	0.15	0.70	
	1	$(H_2+N_2+CH_4+CO)$	1.0	221900.8	98.96			
		CO_2	0.8	2329.6	1.04	1.04	4.83	78.53

Table 7.6A: Collected data at different time as reaction proceeded. Catalyst was not prereduce while temp and composition was constant.

Run No.	Temp. (^{0}C)	Component	Flowrate(ml/min)	%volume
1 to 12	300	CO_2	16	2.6
		N_2	450	73.1
		H_2	150	24.3

Table 7.6B: Collected data at different time as reaction proceeded. Cataltst was not prereduced while temperature and composition was constant.

Run No.	Time (hr.)	Peak Position	COLUMN - 2 H_2	N_2	CH_4	CO	COLUMN - 1 (H_2+N_2+CH_4+CO)	CO_2
1	1	Atn.	32	256	16	2.0	512	4.0
		Ph	70.1	45.6	34.1	35.9	30.2	71.0
		Pw	2.0	7.0	6.0	6.0	11.0	13.8
2	2	Atn.	32	256	16	2.0	512	4.0
		Ph	74.6	45.8	45.7	38.6	33.9	68.0
		Pw	2.0	6.5	5.0	5.5	11.0	13.8
3	3	Atn.	32	256	16	2.0	512	4.0
		Ph	74.7	36.3	50.1	38.8	37.0	65.5
		Pw	2.0	6.5	5.0	5.5	11.0	13.5
4	4	Atn.	32	256	16	2.0	512.0	4.0
		Ph	75.0	47.0	56.3	39	41.5	61.6
		Pw	2.0	6.5	5.0	5.6	11.0	13.5
5	5	Atn.	32	256	16	1.0	512	4.0
		Ph	76.7	49.0	61.9	36.0	41.5	55.6
		Pw	2.0	6.5	5.0	5.5	11.0	13.0
6	6	Atn.	32	256	16	1.0	512	4.0
		Ph	83.3	50.5	65.9	34.8	39.8	46.7
		Pw	2.0	7.0	5.5	5.5	11.0	13.0

Run No.	Time (hr.)	Peak Position	COLUMN - 2				COLUMN - 1	
			H_2	N_2	CH_4	CO	(H_2+N_2+CH_4+CO)	CO_2
		Atn.	32	256	16	2.0	512	4.0
7	7	Ph	84.3	52.0	77.5	34.0	39.5	43.3
		Pw	2.0	7.0	5.5	5.5	11.0	12.5
		Atn.	32	256	16	2.0	512	4.0
8	8	Ph	85.5	53.2	75.6	26.5	39.0	41.5
		Pw	2.0	7.0	6.0	6.0	11.0	12.0
		Atn.	32	256	16	2.0	512	4.0
9	9	Ph	87.5	54.7	81.0	44.0	39.0	40.0
		Pw	2.0	7.0	6.0	6.0	11.0	12.0
		Atn.	32	256	16	2.0	512.0	4.0
10	10	Ph	87.7	56.0	84.8	45.8	37.0	36.6
		Pw	2.0	7.0	6.0	6.0	11.0	12.0
		Atn.	32	256	16	1.0	512	4.0
11	11	Ph	88.4	57.5	89.8	41.0	37.0	36.6
		Pw	2.0	7.0	6.0	6.0	11.0	12.0
		Atn.	32	256	16	1.0	512	4.0
12	12	Ph	88.4	57.5	89.8	41.0	37.0	36.6
		Pw	2.0	7.0	6.0	6.0	11.0	12.0

Run No.	Column	Component	k_f	Area	%Volume in each col. (dry basis)	%Volume in outlet (dry basis)	Component flow rate (ml/min)	$\%CO_2$ Conv.
4	2	H_2	36.00	172800.00	67.50	66.74	331.38	
		N_2	1.00	78208.00	30.55	30.21	150.00	
		CH_4	1.00	4500.00	1.76	1.74	8.64	
		CO	1.13	493.58	0.19	0.19	0.94	
	1	$(H_2+N_2+CH_4+CO)$	1.00	233728.00	98.88			
		CO_2	0.80	2661.12	1.12	1.12	5.56	65.25
5	2	H_2	36.00	161510.40	68.65	67.40	343.20	
		N_2	1.00	70584.30	30.00	29.00	150.00	
		CH_4	1.00	4952.00	1.88	1.86	9.10	
		CO	1.13	447.48	0.17	0.17	0.83	
	1	$(H_2+N_2+CH_4+CO)$	1.00	233728.00	99.02			
		CO_2	0.80	2313.00	0.98	0.98	4.80	70.0
6	2	H_2	36.00	191923.20	66.49	65.92	318.10	
		N_2	1.00	90496.00	31.35	31.08	150.00	
		CH_4	1.00	5799.20	2.01	1.99	9.60	
		CO	1.13	432.50	0.15	0.15	0.72	
	1	$(H_2+N_2+CH_4+CO)$	1.00	224153.60	99.14			
		CO_2	0.80	1942.70	0.86	0.86	4.15	74.1

Run No.	Column	Component	k_i	Area	%Volume in each col. (dry basis)	%Volume in outlet (dry basis)	Component flow rate (ml/min)	$\%CO_2$ Conv.
		H_2	36.00	172800.00	67.50	66.74	331.38	
		N_2	1.00	78208.00	30.55	30.21	150.00	
4	2	CH_4	1.00	4500.00	1.76	1.74	8.64	
		CO	1.13	493.58	0.19	0.19	0.94	
	1	$(H_2+N_2+CH_4+CO)$	1.00	233728.00	98.88			
		CO_2	0.80	2661.12	1.12	1.12	5.56	65.25
		H_2	36.00	161510.40	68.65	67.40	343.20	
		N_2	1.00	70584.30	30.00	29.00	150.00	
5	2	CH_4	1.00	4952.00	1.88	1.86	9.10	
		CO	1.13	447.48	0.17	0.17	0.83	
	1	$(H_2+N_2+CH_4+CO)$	1.00	233728.00	99.02			
		CO_2	0.80	2313.00	0.98	0.98	4.80	70.0
		H_2	36.00	191923.20	66.49	65.92	318.10	
		N_2	1.00	90496.00	31.35	31.08	150.00	
6	2	CH_4	1.00	5799.20	2.01	1.99	9.60	
		CO	1.13	432.50	0.15	0.15	0.72	
	1	$(H_2+N_2+CH_4+CO)$	1.00	224153.60	99.14			
		CO_2	0.80	1942.70	0.86	0.86	4.15	74.1

Run No.	Column	Component	k_i	Area	%Volume in each col.	%Volume in outlet	Component flow rate	%CO_2 Conversion
7	2	H_2	36.00	194227.20	65.92	65.41	312.67	
		N_2	1.00	93184.00	31.62	31.38	150.00	
		CH_4	1.00	6820.00	2.31	2.29	10.95	
		CO	1.13	422.62	0.14	0.14	0.67	
	1	(H_2+N_2+CH_4+CO)	1.00	222464.00	99.23			
		CO_2	0.80	1732.00	0.77	0.77	3.68	77
8	2	H_2	36.00	196992.00	65.68	65.21	310.00	
		N_2	1.00	95334.40	31.78	31.55	150.00	
		CH_4	1.00	7257.60	2.42	2.40	11.41	
		CO	1.13	359.30	0.12	0.12	0.57	
	1	(H_2+N_2+CH_4+CO)	1.00	219739.70	99.28			
		CO_2	0.80	1593.60	0.72	0.72	3.42	78.6
9	2	H_2	36.00	201600.00	65.51	66.06	308.40	
		N_2	1.00	980224.00	31.86	31.64	150.00	
		CH_4	1.00	7776.00	2.53	2.51	11.90	
		CO	1.13	298.32	0.10	0.10	0.47	
	1	(H_2+N_2+CH_4+CO)	1.00	219648.00	99.31			
		CO_2	0.80	1536.00	0.69	0.69	3.27	79.6

Run No.	Column	Component	k_f	Area	%Volume in each col. (dry basis)	%Volume in outlet (dry basis)	Component flow rate (ml/min)	$\%CO_2$ Conv.
10	2	H_2	36.00	202060.80	65.00	64.56	302.00	
		N_2	1.00	100352.00	32.28	32.06	150.00	
		CH_4	1.00	8140.80	2.62	2.60	12.21	
		CO	1.13	310.50	0.10	0.10	0.47	
	1	$(H_2+N_2+CH_4+CO)$	1.00	208384.00	99.33			
		CO_2	0.80	1405.44	0.67	0.67	3.13	80.4
11	2	H_2	36.00	203558.40	64.52	64.09	296.35	
		N_2	1.00	103040.00	32.66	32.44	150.00	
		CH_4	1.00	8620.80	2.73	2.71	12.53	
		CO	1.13	277.98	0.09	0.09	0.42	
	1	$(H_2+N_2+CH_4+CO)$	1.00	208384.00	99.33			
		CO_2	0.80	1405.44	0.67	0.67	3.10	80.6
12	2	H_2	36.00	203558.40	64.52	64.09	296.35	
		N_2	1.00	103040.00	32.66	32.44	150.00	
		CH_2	1.00	8620.80	2.73	2.71	12.53	
		CO	1.13	278.00	0.09	0.09	0.42	
	1	$(H_2+N_2+CH_4+CO)$	1.00	208384.00	99.33			
		CO_2	0.80	1405.40	0.67	0.67	3.10	80.6

Table 7.7: Data of ln(x) corresponding temperature for 2.6% inlet carbon dioxide concentration

$T(^0C)$	x	ln(x)	$(1/T)X10^3$ K^{-1}	Activation Energy, Ea (KCal/gmol)
210	0.6525	-0.4269	2.07	
220	0.683	-0.3813	2.03	
230	0.730	-0.3147	1.99	2.54
240	0.770	-0.2614	1.95	
250	0.796	-0.228	1.91	
300	0.806	-0.2156	1.74	

Table 7.8: Data of ln(x) corresponding temperature for 3.6% inlet carbon dioxide concentration

$T(^0C)$	x	ln(x)	$(1/T)X10^3$ K^{-1}	Activation Energy, Ea (KCal/gmol)
210	0.646	-0.4369	2.07	
220	0.672	-0.3975	2.03	
230	0.715	-0.3355	1.99	2.52
240	0.747	-0.2917	1.95	
250	0.76	-0.2744	1.91	
300	0.7853	-0.2417	1.74